Advanced Powder Technology xxx (xxxx) xxx

Contents lists available at ScienceDirect

Advanced Powder Technology

journal homepage: www.elsevier.com/locate/apt

Original Research Paper

# Mixed convection of non-Newtonian nanofluid in an H-shaped cavity with cooler and heater cylinders filled by a porous material: Two phase approach

Zhixiong Li [a,b], Pouya Barnoon [c], Davood Toghraie [c], Reza Balali Dehkordi [d], Masoud Afrand [e,f,*]

[a] Ocean College, Minjiang University, Fuzhou 350108, China
[b] Key Laboratory of Fluid Power and Intelligent Electro-Hydraulic Control (Fuzhou University), Fujian Province University, Fuzhou 350108, China
[c] Young Researchers and Elite Club, Khomeinishahr Branch, Islamic Azad University, Khomeinishahr, Iran
[d] Senior Operations and Executives Engineer of Oil Terminal Company, Kharg Island, Iran
[e] Laboratory of Magnetism and Magnetic Materials, Advanced Institute of Materials Science, Ton Duc Thang University, Ho Chi Minh City, Viet Nam
[f] Faculty of Applied Sciences, Ton Duc Thang University, Ho Chi Minh City, Viet Nam

ARTICLE INFO

*Article history:*
Received 12 May 2019
Received in revised form 27 July 2019
Accepted 13 August 2019
Available online xxxx

*Keywords:*
Two phase
H-shaped
Mixed convection
Porous
Cooler and heater cylinders

ABSTRACT

In the present problem, two-phase mixed convection of a non-Newtonian nanofluid in a porous H-shaped cavity is studied. Inside the enclosure there are four rotating cylinders, using the Boussinesq approximation, mixed convection is created. Nanofluid includes $H_2O$ + 0.5% CMC and copper oxide nanoparticles. The mixture model was used to model physical phenomena. Different aspect ratios were used in order to achieve the best heat transfer rate. The Darcy and Richardson numbers ranges are $10^{-4} \leq Da \leq 10^{-2}$ and $1 \leq Ri \leq 100$ respectively. Also, the aspect ratio and dimensionless angular velocities of cylinders ranges are $1.4 \leq AR \leq 1.6$ and $-10 \leq \Omega \leq 10$ respectively. Streamlines and isotherm-lines contours have been obtained for the variation of Darcy and Richardson numbers, aspect ratio and angular velocity. The heat transfer rates have been obtained for various aspect ratios, Darcy and Richardson numbers, and the direction of the cylinder's rotation, and are compared with each other. The results show that the direction of cylinders rotation influences the strength and extent of the generation vortices. Also, the use of porous material in high permeability can be a good alternative to lowering the angular velocity of the cylinders and ultimately reducing the need for less energy.



## 1. Introduction

After discovering nanofluids and demonstrating the remarkable improvement in their thermo-physical properties at low concentrations, many factories, and research groups have tried to employ them in new systems and equipment in various sciences such as electronics, transportation, medicine, aerospace and etc. [1–3]. The use of mechanisms such as nanofluids and the porous medium or the change in the geometry structure can help improve heat transfer [4–6]. The analysis of nanofluid heat transfer and entropy generation in a cavity was investigated by Mehrez et al. [7]. They found that the heat transfer and the entropy generation vary with the aspect ratio of the cavity and nanoparticle types. Ahmed et al. [8] investigated natural convection heat transfer in a trapezoidal cavity with a porous medium. A similar study was conducted with the help of the LBM by Abadshapoori and Saidi [9]. Al-Srayyih et al. [10] studied the effect of a linearly heated left sidewall on natural convection flows in a porous cavity. They concluded that the nanofluid produces more enhancement of heat transfer compared to the base fluid. Emami et al. [11] studied the natural convection of nanofluid in an inclined porous cavity. They found that use of nanofluid with porous media is beneficial. Heat transfer enhancement of mixed convection in an inclined porous cavity using nanofluid was studied by Rajarathinam et al. [12]. Also, Hashim et al. [13] investigated the natural convection of alumina-water nanofluid in a wavy cavity. They found that the heat transfer inside the cavity is enhanced by introducing nanoparticles as well as a selection of the optimal number of oscillations. Cheng [14] studied the mixed convection heat transfer and entropy generation of nanofluid in wavy wall lid-driven cavity. They found that the mean Nusselt number and total entropy generation increase with an increasing Richardson number and Reynolds number. Buongiorno's

* Corresponding author at: Ton Duc Thang University, Ho Chi Minh City, Viet Nam.
*E-mail address:* masoud.afrand@tdtu.edu.vn (M. Afrand).

https://doi.org/10.1016/j.apt.2019.08.014
0921-8831/

## Nomenclature

| | |
|---|---|
| Da | Darcy number $\left(=\kappa/L^2\right)$ |
| $C_p$ | specific heat capacity $\left[\frac{j}{kg\ K}\right]$ |
| D(=2R) | diameter of cylinder [m] |
| $f_{drag}$ | drag function |
| g | acceleration due to gravity $\left[\frac{m}{s^2}\right]$ |
| Gr | Grashof number $\left(=\frac{g\beta_f \Delta T L^3}{\nu_f^2}\right)$ |
| L | length of cavity [m] |
| k | Thermal conductivity $\left[\frac{W}{m\ K}\right]$ |
| Nu | Local Nusselt number $\left(=\frac{h(x)H}{k}\right)$ |
| h(x) | local heat transfer coefficient $\left(=\frac{q''(x)}{T_H-T_c}\right)$ |
| $q''$ | heat flux $\left(=\frac{1}{H}\int_0^H q''(x)dx\right)\left[\frac{W}{m^2}\right]$ |
| $Nu_{ave}$ | Average Nusselt number $\left(=\frac{hH}{k}\right)$ |
| h | average heat transfer coefficient $\left(=\frac{q''}{\Delta T}\right)\left[\frac{W}{m^2K}\right]$ |
| R | radius of cylinder [m] |
| Ra | Rayleigh number (= Gr.Pr) |
| Pr | Prandtl number |
| T | Temperature [K] |
| u, v | Velocity components $\left[\frac{m}{s}\right]$ |
| X | Dimensionless length in × direction (= x/H) |
| Y | dimensional length in y direction (= y/H) |
| n | power-law index |
| K | consistency index [Pa.s$^n$] |
| AR | aspect ratio |

*Greek Symbols*

| | |
|---|---|
| β | thermal expansion coefficient $\left[\frac{1}{K}\right]$ |
| θ | dimensionless temperature |
| ν | kinematic viscosity $\left[\frac{m}{s^2}\right]$ |
| φ | volume fraction |
| Ψ | dimensionless stream function |
| ρ | Density $\left[\frac{kg}{m^3}\right]$ |
| κ | permeability [m$^2$] |
| ε | porosity |
| η | dynamic viscosity $\left[\frac{kg}{m.s}\right]$ |
| $\dot{\gamma}$ | shear rate |

*Super-and sub-scripts*

| | |
|---|---|
| bf | base fluid |
| C | cold |
| dr | drift |
| f | fluid |
| H | hot |
| k | of water of nanofluid |
| m | mixture |
| nf | nanofluid |
| p | particle |
| ave | average |

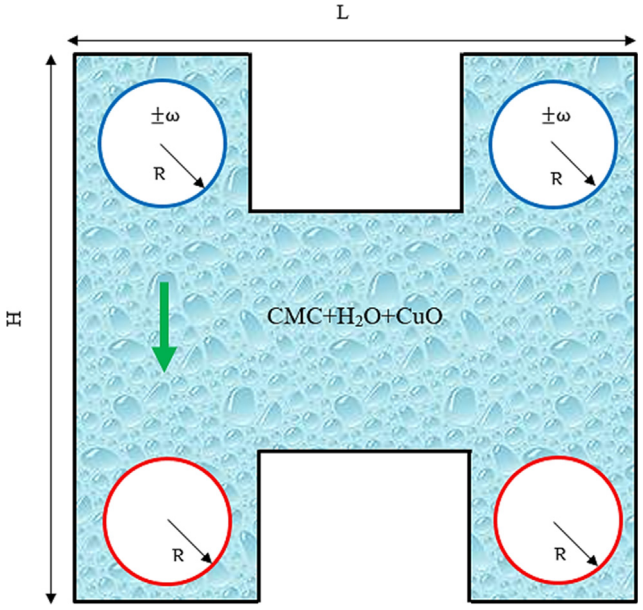


**Fig. 1.** The geometry studied for the present problem.

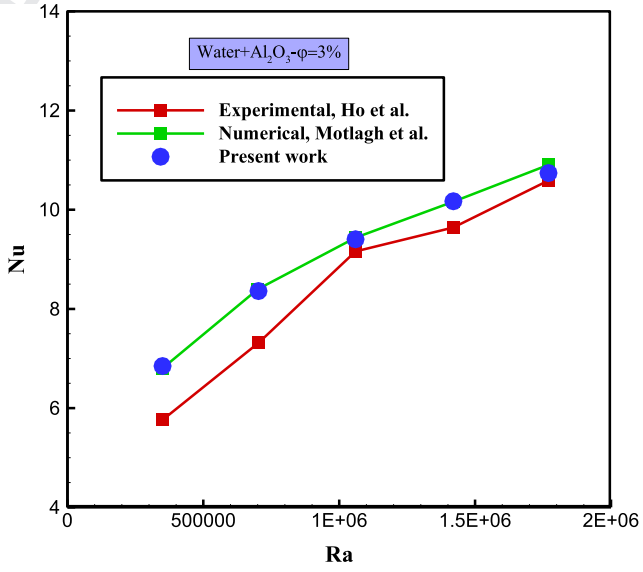


**Fig. 2.** Comparison between present work with Refs. [38,39].

**Table 1**
Grid independency for Ri = 1, Da = $10^{-3}$ and φ = 1%.

| No. | Element | ψ | % Error for ψ | Nu number | % Error for Nu number |
|---|---|---|---|---|---|
| 1 | 33,510 | 29.444 | – | 6.730051 | – |
| 2 | 50,266 | 29.127 | 1.08 | 6.512663 | 3.33 |
| **3** | **75,400** | **29.063** | **0.22** | **6.425467** | **1.35** |
| 4 | 113,100 | 29.056 | 0.024 | 6.398293 | 0.42 |

Please cite this article as: Z. Li, P. Barnoon, D. Toghraie et al., Mixed convection of non-Newtonian nanofluid in an H-shaped cavity with cooler and heater cylinders filled by a porous material: Two phase approach, Advanced Powder Technology, https://doi.org/10.1016/j.apt.2019.08.014

two-phase model and natural convection in a partially heated enclosure were studied by Wang et al. [15]. They observed that at low Rayleigh numbers, the heat transfer enhancement increases in nanoparticle volume fraction. Al-Rashed et al. [16] studied mixed convection in a lid-driven cavity using nanofluid. Baïri [17] investigated natural convection between concentric and inclined hemispherical cavities filled with Cu-water nanofluid. Transient natural convection and entropy generation analysis in a porous cavity filled with nanofluid was studied by Baghsaz et al. [18]. They observed the Nusselt number decreased during the nanoparticle sedimentation process. Other useful studies in this regard can be found in [19–23]. Khalili et al. [24] investigated the non-homogenous distribution of nanoparticles in the nanofluid by natural convection heat transfer inside a square enclosure experimentally. They observed that the average nanoparticle volume fraction along the cold wall is 3.10% greater than that along hot wall. Experimental study of natural convection in enclosures was done by Mahian et al. [25]. They found that even without having measured data of thermophysical properties, the average Nusselt number could be estimated with the same trend and maximum difference of 4.5%. Other useful laboratory studies are found in [26–30]. Other numerical studies in this regard can be found in Refs. [43–62].

In this work, fluid flow and heat transfer are studied in a porous H-shaped cavity using two- phase approach. The use of four rotating cylinders, considering cooler and heater as a useful idea in a porous H-shaped cavity is a distinguishing feature of the present work with other researchers.

## 2. Problem statement

In this study, fluid flow and heat transfer of a non-Newtonian nanofluid in an H-shaped enclosure with rotating obstacles filled by a porous medium are investigated. Two-phase approach is used

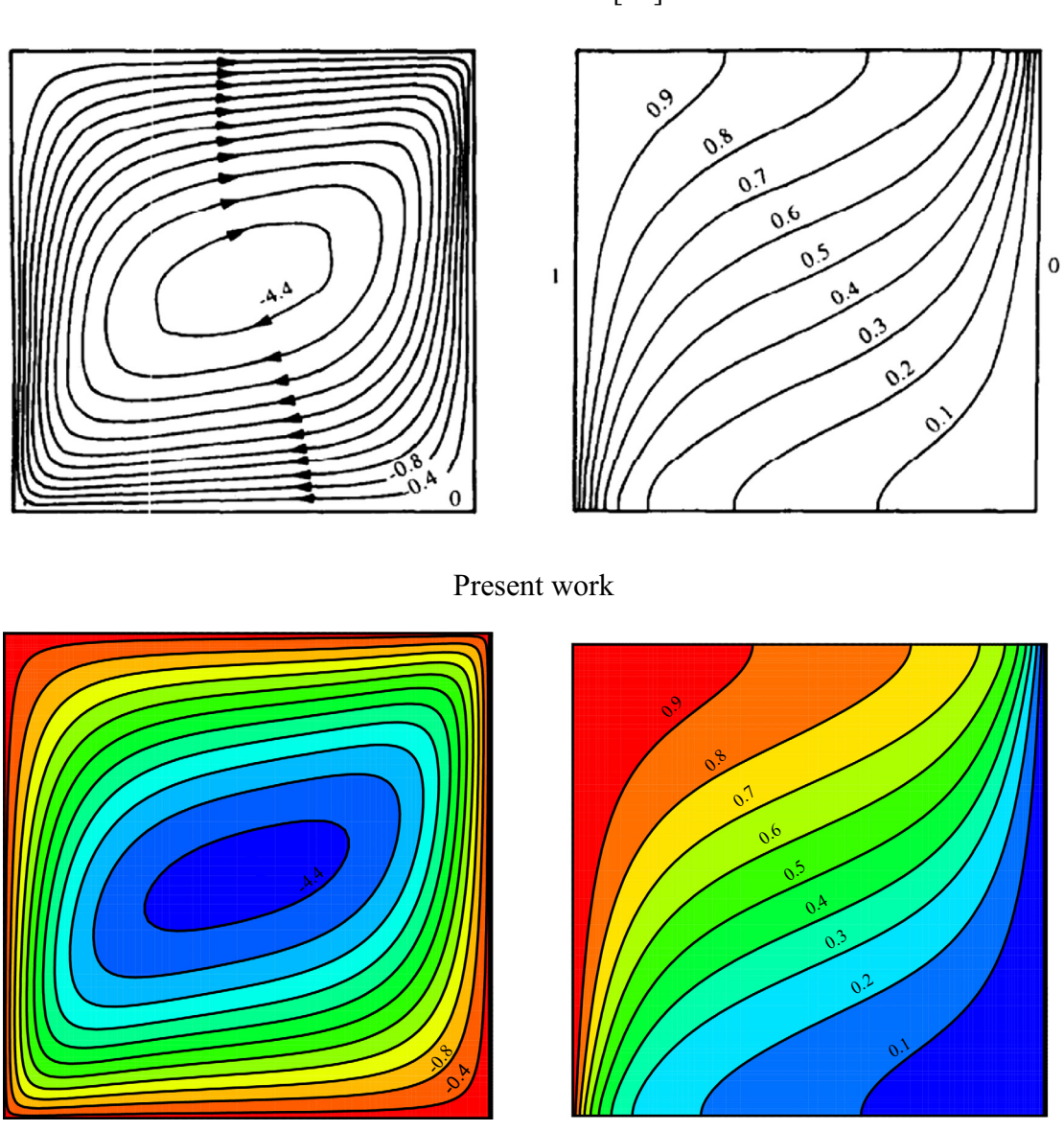


**Fig. 3a.** Comparison between streamlines (left) and isotherm-lines (right) with Ref. [40] for Da = $10^{-6}$, Ra = $10^{8}$, porosity = 0.8.

Please cite this article as: Z. Li, P. Barnoon, D. Toghraie et al., Mixed convection of non-Newtonian nanofluid in an H-shaped cavity with cooler and heater cylinders filled by a porous material: Two phase approach, Advanced Powder Technology, https://doi.org/10.1016/j.apt.2019.08.014

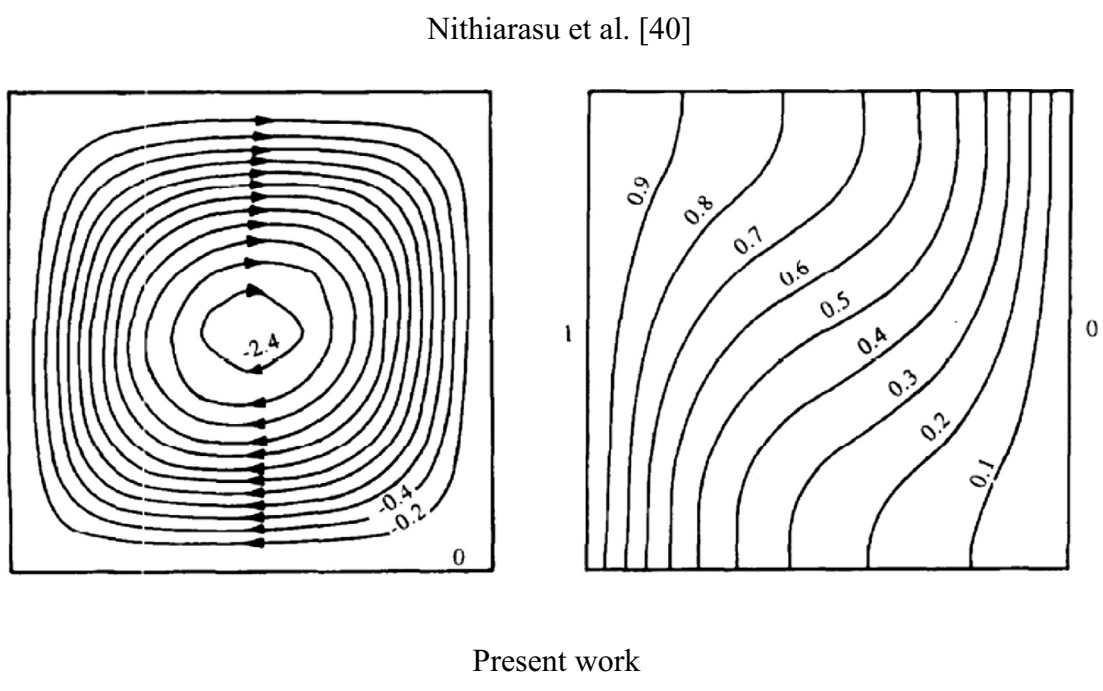


**Fig. 3b.** Comparison between streamlines (left) and isothermlines (right) with Ref. [40] for Da = $10^{-2}$, Ra = $10^4$, porosity = 0.6.

**Table 2**
Thermophysical properties of nanofluid [5,42].

| Type | ρ(kg/m$^3$) | $C_p$(J/kg K) | k(w/m K) |
|---|---|---|---|
| $H_2O$ + CMC | 998.2 | 4182 | 0.6 |
| CuO | 6500 | 540 | 18 |

to model physical phenomena. Four rotating cylinders with the same radiuses (= R) are embedded in the cavity. The dimensions of the cavity are H × L. The schematic of geometry is shown in Fig. 1. The upper and lower cylinders are subjected to cold and hot temperatures respectively. Other walls in the cavity are insulated. The local thermal equilibrium approach for porous media and fluid phase is used. The porous medium is considered homogeneous and anisotropic. The cells of the porous medium are completely open and the size of the pores is sufficiently large compared to the nanoparticles and the molecular diameter of the base fluid. Three different aspect ratios are used to achieve the best heat transfer rate. Carboxy-methylcellulose (CMC) + Water and CuO nanoparticles are used as working fluid. The Richardson and Darcy numbers ranges are $1 \leq Ri \leq 100$ and $10^{-4} \leq Da \leq 10^{-2}$ respectively. In addition, the parameters such as aspect ratio, dimensionless angular velocity and volume fraction ranges are $1.4 \leq AR \leq 1.6$, $-10 \leq \Omega \leq +10$ and $0 \leq \varphi \leq 0.01$ respectively. In this study, the effects of porous medium, angular velocity of cylinders and direction of rotation cylinders on flow pattern and heat transfer are studied.

## 3. Two phase mixture model

The mixture model is simplified with Eulerian's approach. In the mixture model, the mixing momentum equations are solved and relative velocities are defined to determine the phase distribution. This model can be used in multiphase flows in which phases move at various velocities. The application of the mixed model is the fol-

Please cite this article as: Z. Li, P. Barnoon, D. Toghraie et al., Mixed convection of non-Newtonian nanofluid in an H-shaped cavity with cooler and heater cylinders filled by a porous material: Two phase approach, Advanced Powder Technology, https://doi.org/10.1016/j.apt.2019.08.014

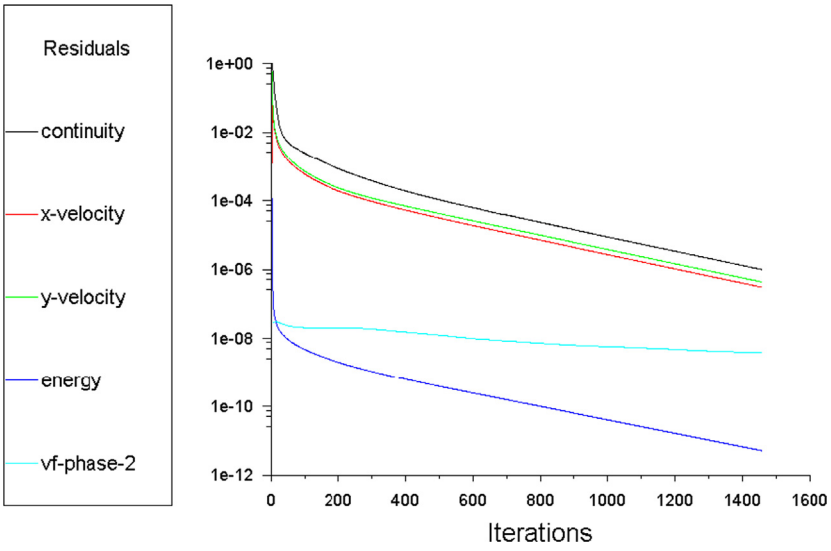


**Fig. 4.** An example of the residuals convergence for the present problem.

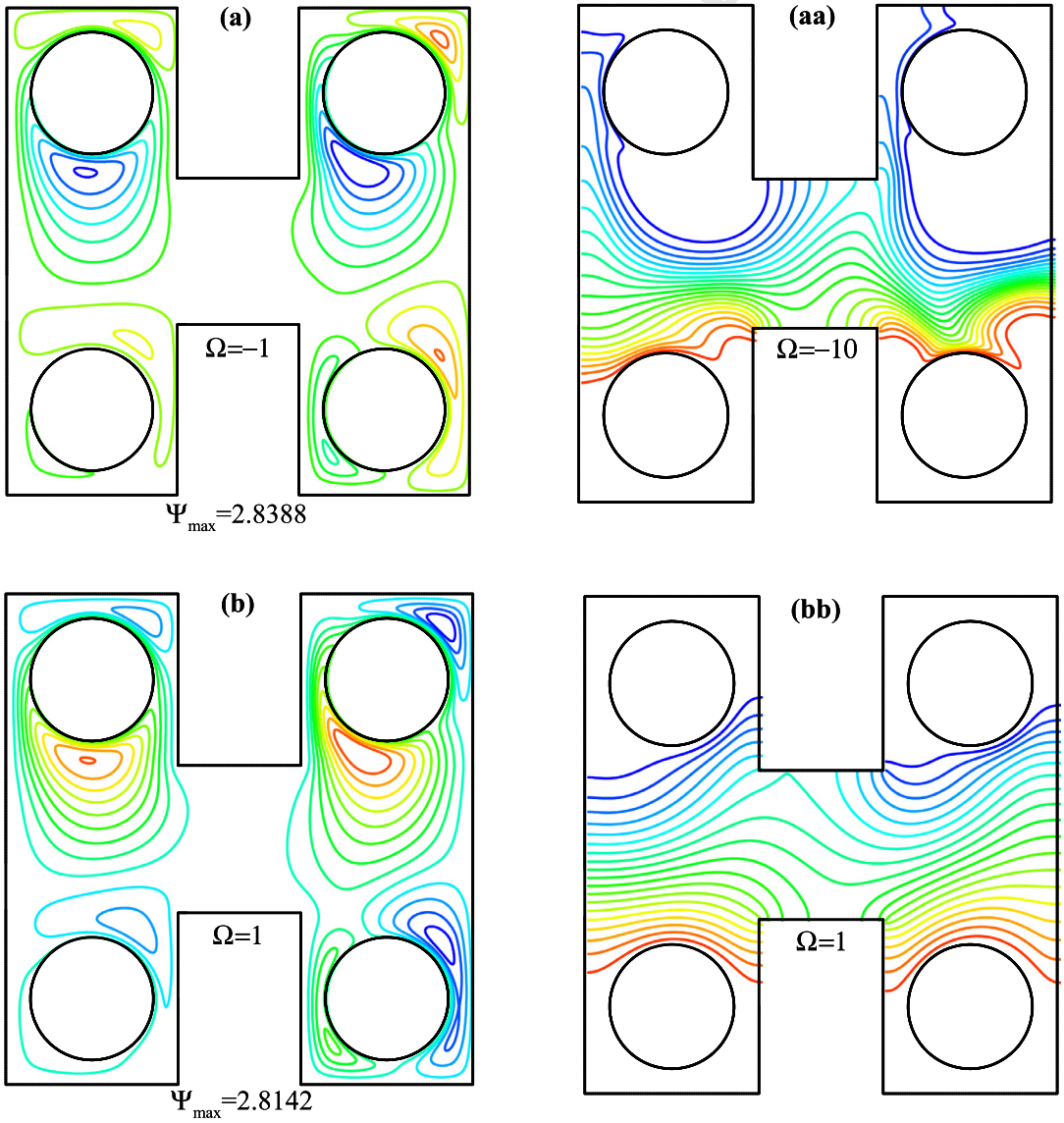


**Fig. 5.** Streamlines (left) and isotherm-lines (right) contours for various dimensioless angular velocities.

Please cite this article as: Z. Li, P. Barnoon, D. Toghraie et al., Mixed convection of non-Newtonian nanofluid in an H-shaped cavity with cooler and heater cylinders filled by a porous material: Two phase approach, Advanced Powder Technology, https://doi.org/10.1016/j.apt.2019.08.014

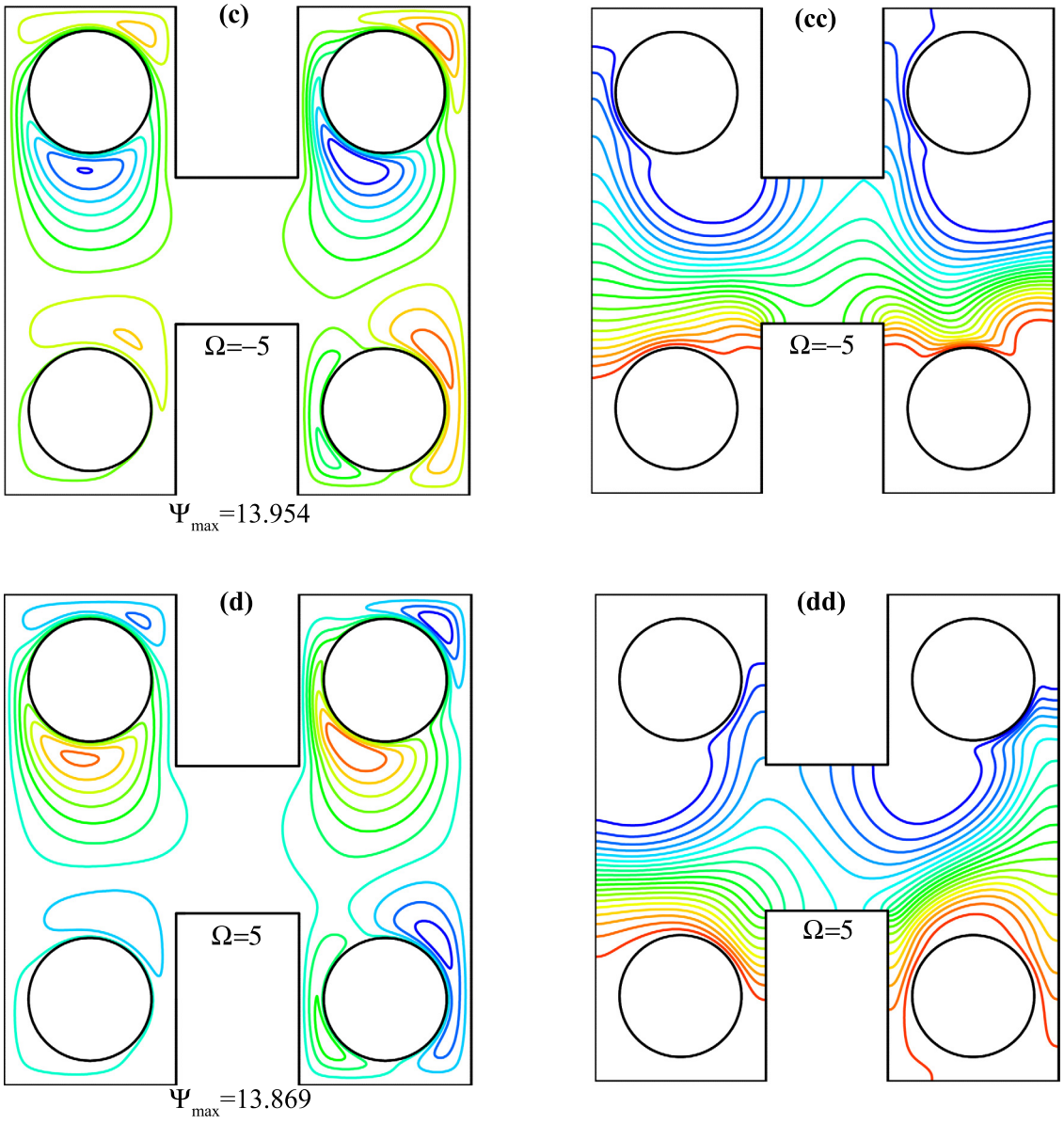


**Fig. 5** (*continued*)

lowing: low pouring stream of particles, bubble flow, sedimentation and silicone separators.

## 4. Govering equations and boundary conditions

*Continuity equation:*

$$\nabla.\left(\rho_m \vec{V}_m\right) = 0 \tag{1}$$

*Momentum equation:*

$$\frac{1}{\varepsilon^2}\nabla.\left(\rho_m \vec{V}_m \otimes \vec{V}_m\right) = -\nabla P + \frac{\eta_m}{\varepsilon}\nabla^2 \vec{V}_m - \frac{\eta_m \vec{V}_m}{\kappa} - \frac{\rho_m C_d}{\sqrt{\kappa}}\vec{V}_m\left|\vec{V}_m\right| - \rho_m \beta_m (T - T_c)g + \nabla.\left(\sum_{k=1}^{n} \varphi_k \rho_k \vec{V}_{dr,k}\vec{V}_{dr,k}\right) \tag{2}$$

Where $\eta_m$ is calculated as follows [5];

$$\eta_m = K(\dot{\gamma})^{n-1} \tag{3}$$

*Energy equation:*

$$\nabla.\left(\sum_{k=1}^{n}(\rho_k C_{p,k})\varphi_k \vec{V}_k T\right) = \nabla.\left(k_m T + \bar{\bar{\tau}}.\vec{V}_m\right) \tag{4}$$

Where in the above equation, we have [5];

$$\bar{\bar{\tau}} = \eta_m\left(\bar{\bar{D}}\right)\bar{\bar{D}} \tag{5}$$

Where;

$$\bar{\bar{D}} = \left(\frac{\partial u_i}{\partial x_j} + \frac{\partial u_j}{\partial x_i}\right) \tag{6}$$

*Volumetric fraction equation:*



Please cite this article as: Z. Li, P. Barnoon, D. Toghraie et al., Mixed convection of non-Newtonian nanofluid in an H-shaped cavity with cooler and heater cylinders filled by a porous material: Two phase approach, Advanced Powder Technology, https://doi.org/10.1016/j.apt.2019.08.014

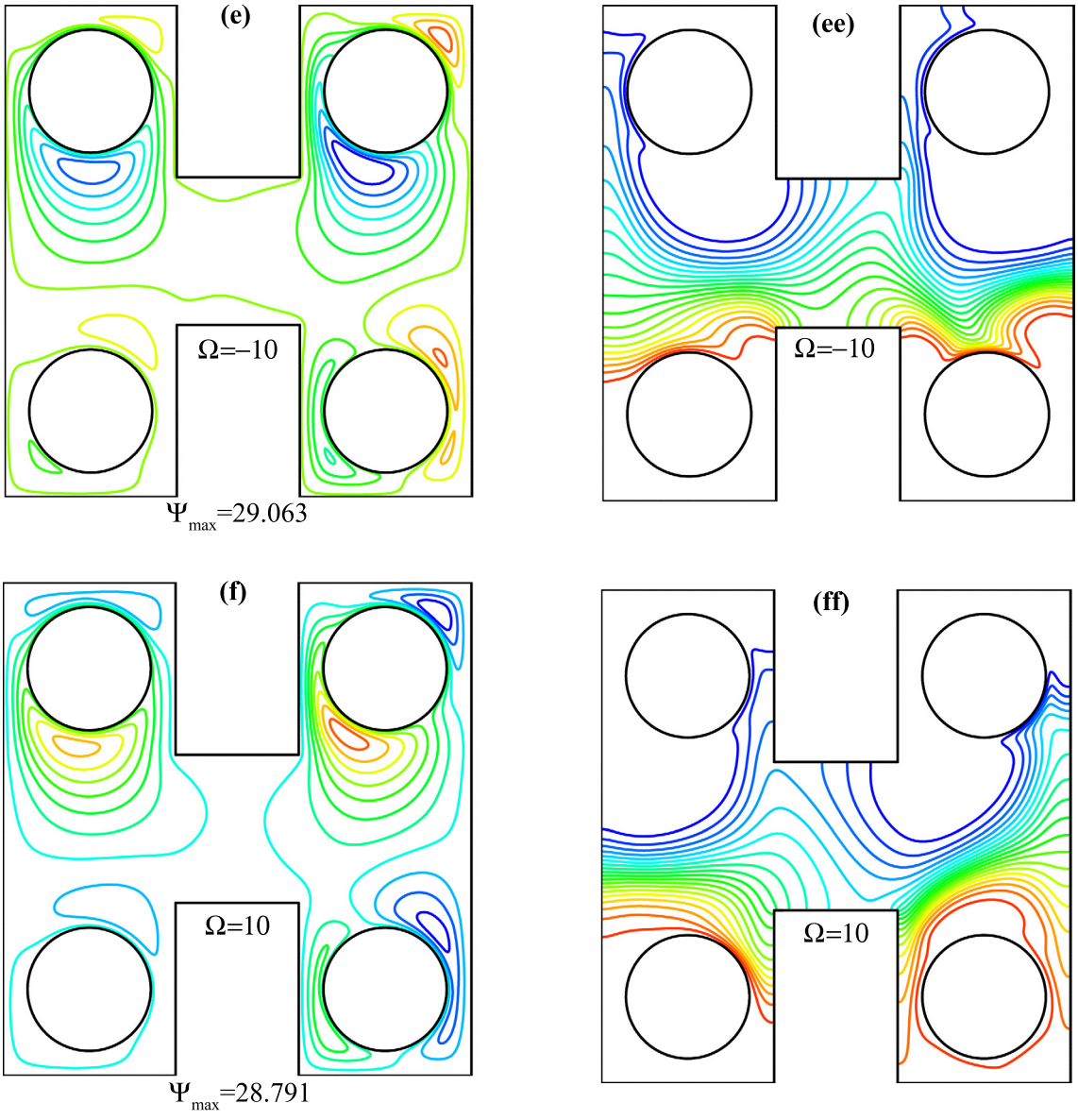


**Fig. 5** (*continued*)

$$\nabla.\left(\varphi_p\rho_p\vec{V}_m\right) = -\nabla.\left(\varphi_p\rho_p\vec{V}_{dr,p}\right) \quad (7)$$

$V_m$ is expressed as [21]:

$$\vec{V}_m = \frac{\sum_{k=1}^{n}\varphi_k\rho_k\vec{V}_k}{\rho_m} \quad (8)$$

Furthermore:

$$\vec{V}_{dr,k} = \vec{V}_k - \vec{V}_m \quad (9)$$

It can be written for slip velocity in the mixture model [21]:

$$\vec{V}_{pf} = \vec{V}_p - \vec{V}_f \quad (10)$$

The drift velocity can be defined as follows. [31]:

$$\vec{V}_{dr,p} = \vec{V}_{pf} - \sum_{k=1}^{n}\frac{\varphi_k\rho_k\vec{V}_{f,k}}{\rho_m} \quad (11)$$

Where:

$$V_{pf} = \frac{\rho_p d_p^2}{18\mu_f f_{drag}}\frac{\left(\rho_p - \rho_m\right)}{\rho_p}(g - (V_m.\nabla)V_m) = V_p - V_f \quad (12)$$

The drag function in the mixture model is expressed as follows [32]:

$$f_{drag} = \begin{cases} 1 + 0.15Re_p^{0.687} & Re_p \le 1000 \\ 0.0183Re_p & Re_p > 1000 \end{cases} \quad (13)$$

The dimensionless forms of governing equations are expressed as follows.

*Continuity equation:*

$$\frac{\partial\bar{u}_m}{\partial\bar{x}} + \frac{\partial\bar{v}_m}{\partial\bar{y}} = 0 \quad (14)$$

*Momentum equation in x-direction:*



Please cite this article as: Z. Li, P. Barnoon, D. Toghraie et al., Mixed convection of non-Newtonian nanofluid in an H-shaped cavity with cooler and heater cylinders filled by a porous material: Two phase approach, Advanced Powder Technology, https://doi.org/10.1016/j.apt.2019.08.014

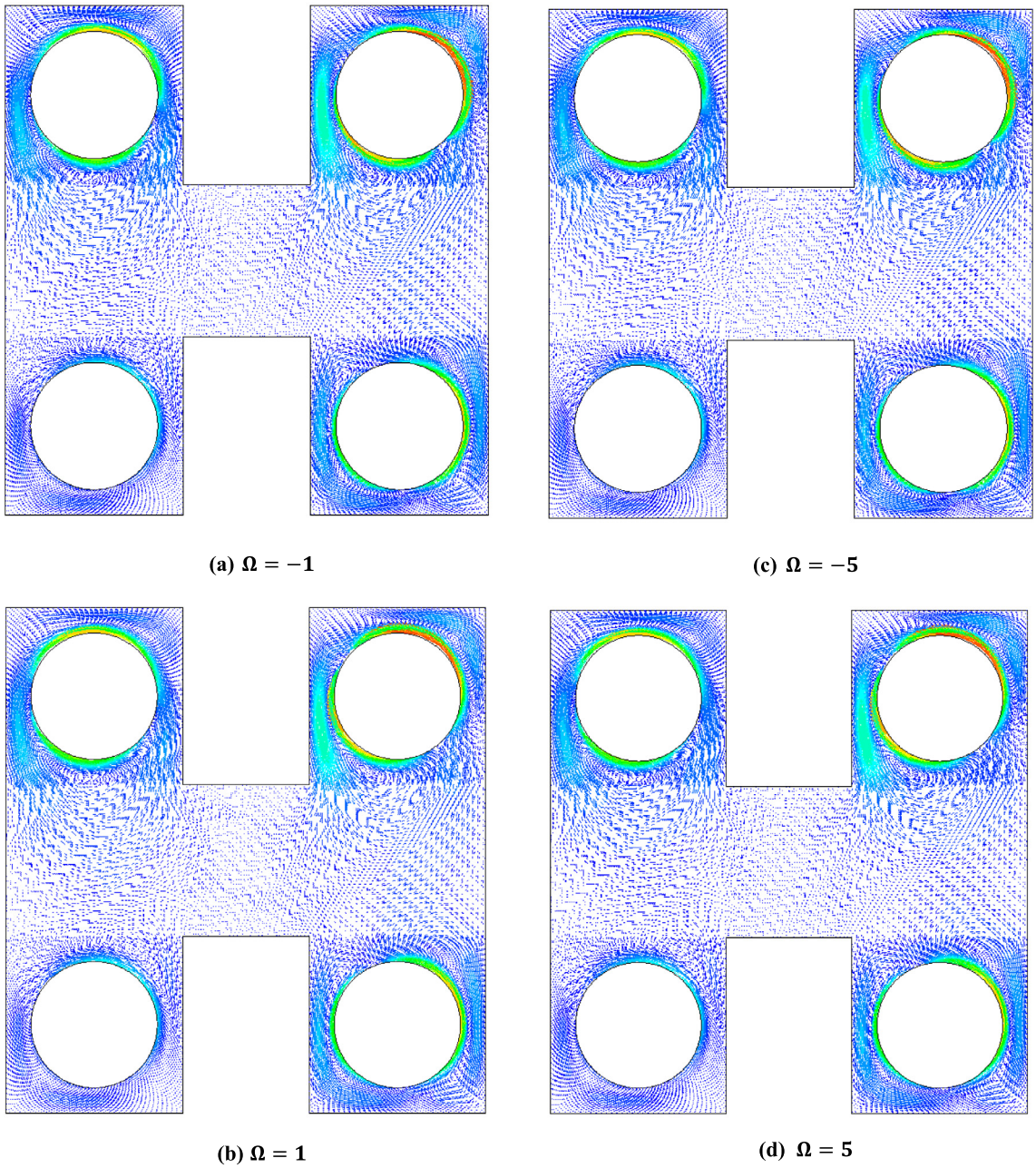


**Fig. 6.** Velocity vectors for Da = $10^{-3}$ and Ri = 100.

$$\left[\bar{u}_m\frac{\partial\bar{u}_m}{\partial\bar{x}}+\bar{v}_m\frac{\partial\bar{u}_m}{\partial\bar{y}}\right]=-\varepsilon^2\frac{\partial\bar{p}_m}{\partial\bar{x}}+\varepsilon\frac{\rho_f}{\rho_m}\left[\frac{\partial}{\partial\bar{x}}\left(Pr\frac{\eta_m}{\eta_f}\frac{\partial\bar{u}_m}{\partial\bar{x}}\right)+\frac{\partial}{\partial\bar{y}}\left(Pr\frac{\eta_m}{\eta_f}\frac{\partial\bar{u}_m}{\partial\bar{y}}\right)\right]-\varepsilon^2\frac{Pr}{Da}\frac{\rho_f}{\rho_m}\frac{\eta_m}{\eta_f}\bar{u}_m-\frac{1.75}{\sqrt{150}}\frac{\varepsilon^{0.5}}{\sqrt{Da}}\bar{u}_m\times\sqrt{\bar{u}_m^2+\bar{v}_m^2}+\varepsilon^2(1-\varphi)\frac{\rho_f}{\rho_m}\left[\bar{u}_{dr,f}\frac{\partial\bar{u}_{dr,f}}{\partial\bar{x}}+\bar{v}_{dr,f}\frac{\partial\bar{u}_{dr,f}}{\partial\bar{y}}\right]+\varepsilon^2\varphi\frac{\rho_p}{\rho_m}\left[\bar{u}_{dr,f}\frac{\partial\bar{u}_{dr,p}}{\partial\bar{x}}+\bar{v}_{dr,p}\frac{\partial\bar{u}_{dr,p}}{\partial\bar{y}}\right] \quad (15a)$$

*Momentum equation in y-direction:*

$$\left[\bar{u}_m\frac{\partial\bar{v}_m}{\partial\bar{x}}+\bar{v}_m\frac{\partial\bar{v}_m}{\partial\bar{y}}\right]=-\varepsilon^2\frac{\partial\bar{p}_m}{\partial\bar{y}}+\varepsilon\frac{\rho_f}{\rho_m}\left[\frac{\partial}{\partial\bar{x}}\left(Pr\frac{\eta_m}{\eta_f}\frac{\partial\bar{v}_m}{\partial\bar{x}}\right)+\frac{\partial}{\partial\bar{y}}\left(Pr\frac{\eta_m}{\eta_f}\frac{\partial\bar{v}_m}{\partial\bar{y}}\right)\right]-\varepsilon^2\frac{Pr}{Da}\frac{\rho_f}{\rho_m}\frac{\eta_m}{\eta_f}\bar{v}_m-\frac{1.75}{\sqrt{150}}\frac{\varepsilon^{0.5}}{\sqrt{Da}}\bar{v}_m\times\sqrt{\bar{u}_m^2+\bar{v}_m^2}+\varepsilon^2(1-\varphi)\frac{\rho_f}{\rho_m}\left[\bar{u}_{dr,f}\frac{\partial\bar{v}_{dr,f}}{\partial\bar{x}}+\bar{v}_{dr,f}\frac{\partial\bar{v}_{dr,f}}{\partial\bar{y}}\right]+\varepsilon^2\frac{(\rho\beta)_m}{(\rho\beta)_f}\frac{\rho_f}{\rho_m}RaPr\theta \quad (15b)$$

Please cite this article as: Z. Li, P. Barnoon, D. Toghraie et al., Mixed convection of non-Newtonian nanofluid in an H-shaped cavity with cooler and heater cylinders filled by a porous material: Two phase approach, Advanced Powder Technology, https://doi.org/10.1016/j.apt.2019.08.014

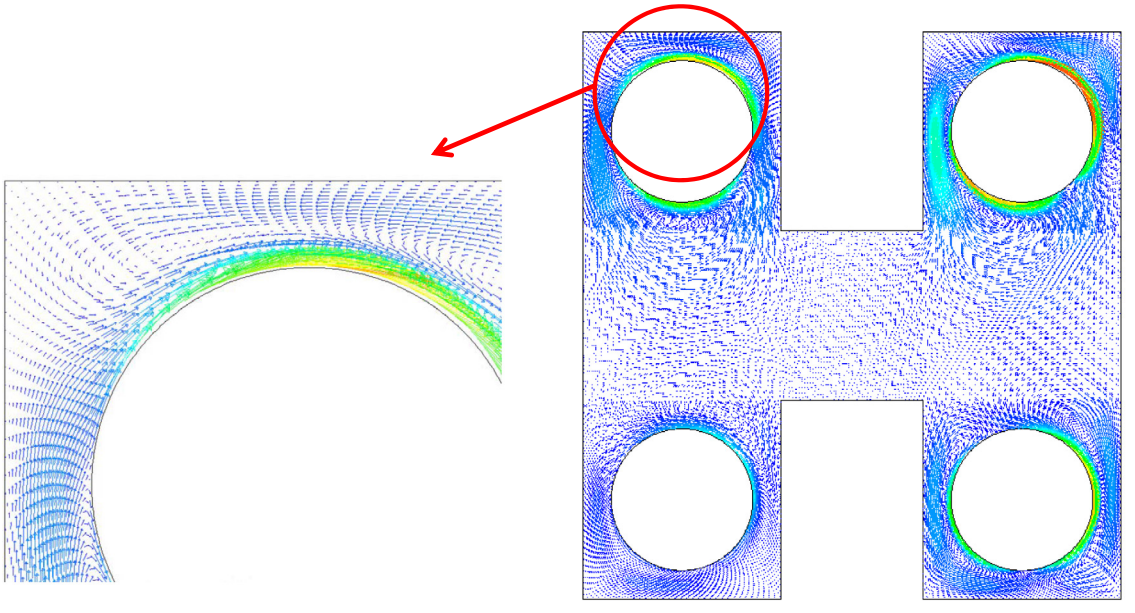

(e) $\Omega = -10$

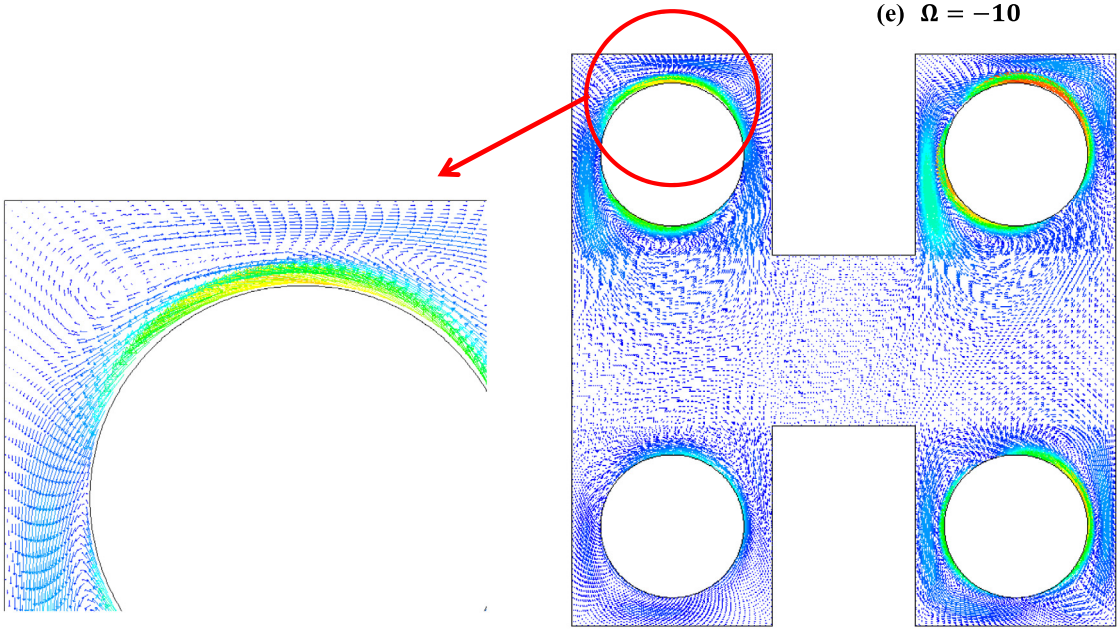

(f) $\Omega = 10$

**Fig. 6** (*continued*)

*Energy equation;*

$$\frac{\rho_p}{\rho_f}\frac{C_{p,p}}{C_{p,f}}\left[\bar{u}_p\frac{\partial}{\partial\bar{x}}(\varphi\theta)+\bar{v}_p\frac{\partial}{\partial\bar{y}}(\varphi\theta)\right]+\left[\bar{u}_f\frac{\partial}{\partial\bar{x}}(1-\varphi)\theta+\bar{v}_f\frac{\partial}{\partial\bar{y}}(1-\varphi)\theta\right]=\frac{\partial}{\partial\bar{x}}\left(\frac{k_m}{k_f}\frac{\partial\theta}{\partial\bar{x}}\right)+\frac{\partial}{\partial\bar{y}}\left(\frac{k_m}{k_f}\frac{\partial\theta}{\partial\bar{y}}\right)+\frac{\partial}{\partial\bar{x}}\frac{\partial\bar{u}_m}{\partial\bar{x}}+\frac{\partial}{\partial\bar{y}}\frac{\partial\bar{v}_m}{\partial\bar{y}} \quad (16)$$

*Volume fraction equation:*

$$\frac{\partial(\varphi\bar{u}_m)}{\partial\bar{x}}+\frac{\partial(\varphi\bar{v}_m)}{\partial\bar{y}}+\frac{\partial(\varphi\bar{u}_{dr,p})}{\partial\bar{x}}+\frac{\partial(\varphi\bar{v}_{dr,p})}{\partial\bar{y}}=0 \quad (17)$$

The thermo-physical properties of the nanofluid are determined according to Eqs. (18)–(21). [33–36]:

$$\rho_m=\rho_f(1-\varphi)+\rho_p\varphi \quad (18)$$

$$(\rho C_p)_m=(\rho C_p)_f(1-\varphi)+(\rho C_p)_p\varphi \quad (19)$$

$$(\rho\beta)_m=(\rho\beta)_f(1-\varphi)+(\rho\beta)_p\varphi \quad (20)$$

$$k_m=k_f\frac{k_p+2k_f+2\varphi(k_p-k_f)}{k_p+2k_f-\varphi(k_p-k_f)} \quad (21)$$

Please cite this article as: Z. Li, P. Barnoon, D. Toghraie et al., Mixed convection of non-Newtonian nanofluid in an H-shaped cavity with cooler and heater cylinders filled by a porous material: Two phase approach, Advanced Powder Technology, https://doi.org/10.1016/j.apt.2019.08.014

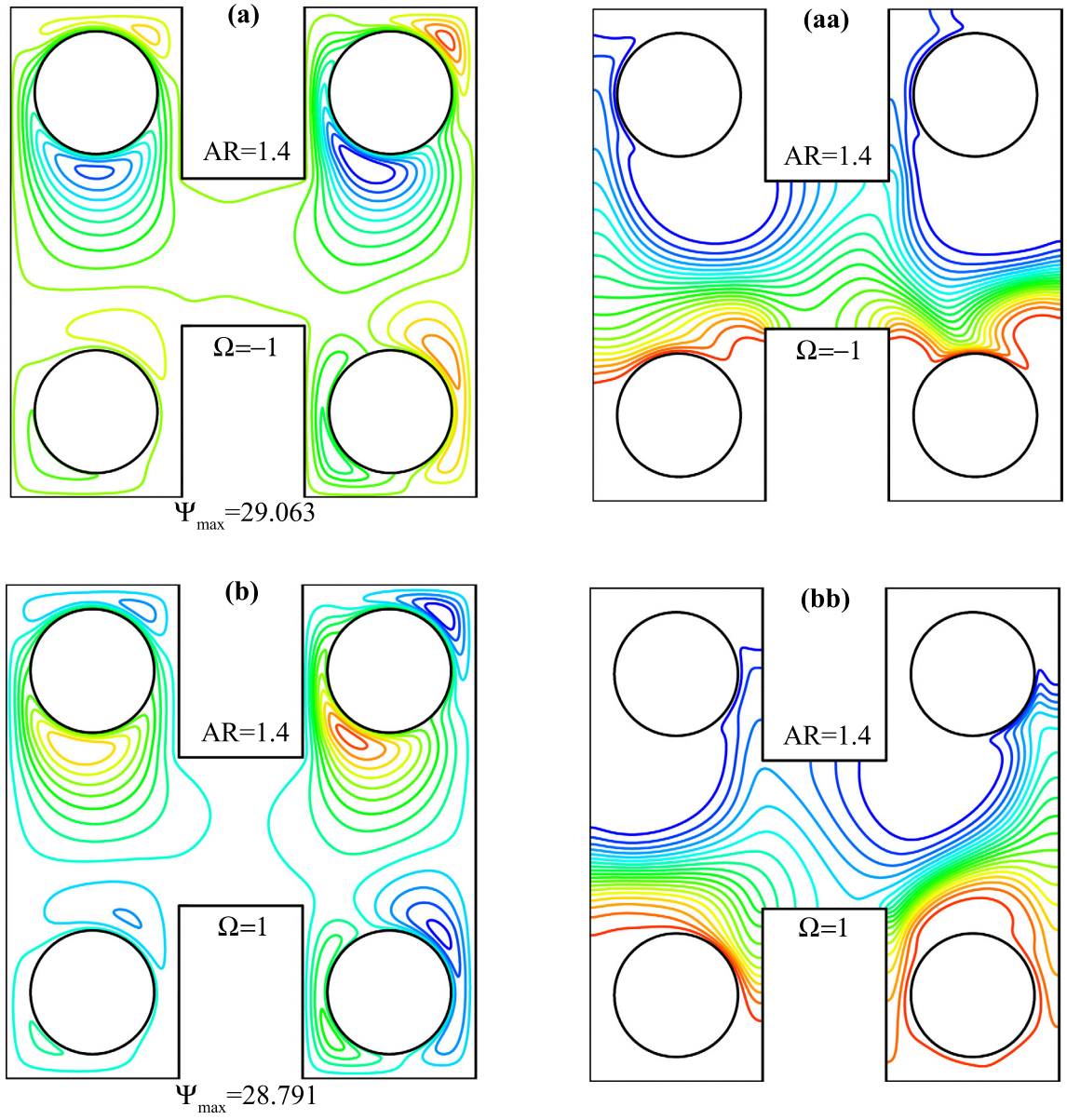


**Fig. 7.** Streamlines (left) and isotherm-lines (right) contours for various aspect ratios.

The dimensionless parameters are expressed as [5,21,37]:

$$\mathrm{Re} = \frac{\rho_f u H}{\mu_f} \tag{22}$$

$$\mathrm{Gr} = \frac{g\beta_f \Delta T H^3}{\nu_f^2} \tag{23}$$

$$\mathrm{Ri} = \frac{\mathrm{Gr}}{\mathrm{Re}^2} \tag{24}$$

$$\mathrm{Da} = \frac{\kappa}{H^2} \tag{25}$$

$$\mathrm{Pr} = \frac{\nu}{\alpha} \tag{26}$$

$$\Omega = \frac{\mp \omega H}{2u_m} \tag{27}$$

$$\theta = \frac{T - T_C}{T_H - T_C} \tag{28}$$

$$B = \frac{2u_m H}{\alpha} \tag{29}$$

$$\bar{x} = \frac{x}{H} \tag{30}$$



Please cite this article as: Z. Li, P. Barnoon, D. Toghraie et al., Mixed convection of non-Newtonian nanofluid in an H-shaped cavity with cooler and heater cylinders filled by a porous material: Two phase approach, Advanced Powder Technology, https://doi.org/10.1016/j.apt.2019.08.014

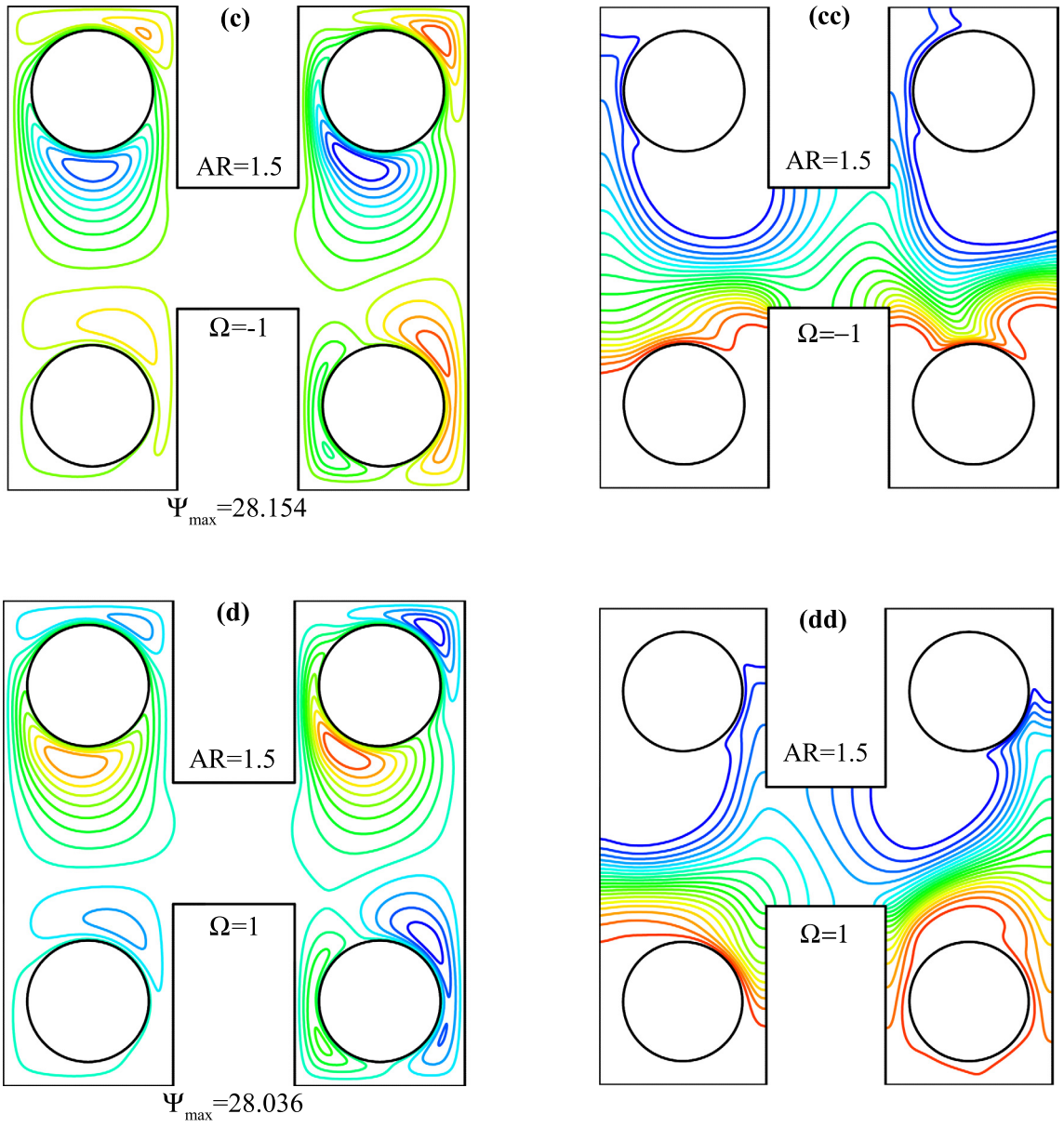


**Fig. 7** (*continued*)

$$\bar{y} = \frac{y}{H} \tag{31}$$

$$P = \frac{p}{\rho_m(\alpha/H)^2} \tag{32}$$

$$\bar{u}_m = \frac{u_m}{\alpha/H} \tag{33}$$

$$\bar{v}_m = \frac{v_m}{\alpha/H} \tag{34}$$

The local Nusselt number is defined as [21]:

$$Nu(x) = \frac{h(x)H}{k} \tag{35}$$

The average convection heat transfer coefficient is defined as:

$$h(x) = \frac{q''(x)}{T_H - T_c} \tag{36}$$

By integrating $q''(x)$, we have [21].

$$q'' = \frac{1}{H}\int_0^H q''(x)dx \tag{37}$$

Therefore, the average parameters are defined as follows. [21]:

$$h = \frac{q''}{\Delta T} \tag{38}$$

$$Nu = \frac{hH}{k} \tag{39}$$



Please cite this article as: Z. Li, P. Barnoon, D. Toghraie et al., Mixed convection of non-Newtonian nanofluid in an H-shaped cavity with cooler and heater cylinders filled by a porous material: Two phase approach, Advanced Powder Technology, https://doi.org/10.1016/j.apt.2019.08.014

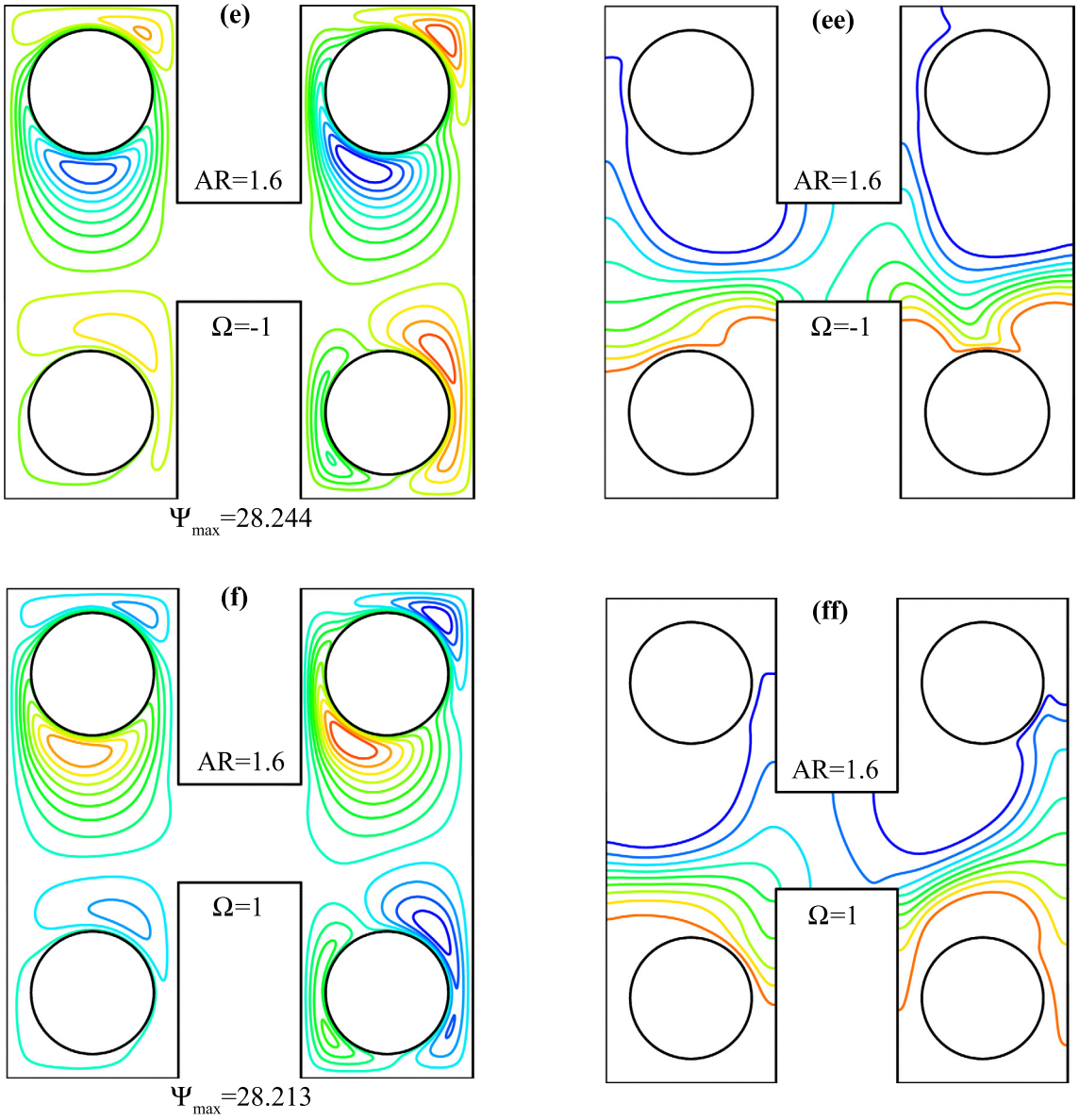


**Fig. 7** (*continued*)

The boundary conditions are expressed as follows;

$$\begin{aligned}
&\text{Adiabaticwalls}: && u_m = v_m = 0, && \tfrac{\partial T}{\partial x} = 0\\
&\text{Coldcylinders}: && u_m = -\omega(y - y_0), && v_m = \omega(x - x_0), \quad T = T_c\\
&\text{Hotcylinders}: && u_m = -\omega(y - y_0), && v_m = \omega(x - x_0), \quad T = T_h
\end{aligned} \tag{40}$$

The dimensionless forms of boundary conditions according to the dimensionless equations are as follows:

$$\begin{aligned}
&\text{Adiabaticwalls}: && \bar{u}_m = \bar{v}_m = 0, && \tfrac{\partial \theta}{\partial \bar{x}} = 0\\
&\text{Coldcylinders}: && \bar{u}_m = -B\Omega\left(\bar{y} - \bar{y}_0\right), && \bar{v}_m = B\Omega\left(\bar{x} - \bar{x}_0\right), \quad \theta = 1\\
&\text{Hotcylinders}: && \bar{u}_m = -B\Omega\left(\bar{y} - \bar{y}_0\right), && \bar{v}_m = B\Omega\left(\bar{x} - \bar{x}_0\right), \quad \theta = 1
\end{aligned} \tag{41}$$

## 5. Grid independency and validation

Four different grids have been used to ensure that results are not dependent on the grid. As shown in Table 1, the ψ and Nu number were used as the criteria for choosing the ultimate mesh. Due to the difference in the result, the third grid has been chosen as the final grid.

Ensuring the numerical solution method is one of the basic criteria for achieving results. For this purpose, two numerical and experimental references are used for comparison. The first validation is related to an experimental study [38]. In an experimental study [38], natural heat transfer was investigated in a cavity with nanofluid. The studied cavity has common conditions and the distribution of nanoparticles is the reason for differences in numerical and laboratory results. For this reason, the results are compared

Please cite this article as: Z. Li, P. Barnoon, D. Toghraie et al., Mixed convection of non-Newtonian nanofluid in an H-shaped cavity with cooler and heater cylinders filled by a porous material: Two phase approach, Advanced Powder Technology, https://doi.org/10.1016/j.apt.2019.08.014

with the same numerical work [39] in this field, details of which are shown in Fig. 2. The small difference in the results shows that the numerical solution method is accurate. The second validation involves comparing the present work with the reference results [40]. Nithiarasu et al. [40] studied the effect of heat transfer in a porous cavity. They used a plurality of porosity to simulate a non-Darcy flow regime. Figs. 3a and 3b show the comparison of the present work with the Ref. [40]. As can be seen, there is a small difference between the results that can be attributed to the numerical solution method and the assumption of Darcy flow instead of non-Darcy flow. Nevertheless, a completely acceptable match between the results can be observed.

## 6. Material properties and problem solving process

Thermophysical properties of nanofluid, such as density, specific heat coefficient and thermal conductivity coefficient according to Table 2, are as follows.

The power-law model is used for the viscosity of nanofluid. In this model, two important parameters k (consistency index) and n (power-law index) are used to calculate viscosity. The values of k and n are calculated Ref. [41]. In this research, the convergence criterion is considered for all cases of $10^{-6}$. Fig. 4 shows an example of the convergence of the residuals for continutiy, velocity, energy, and volume fraction equations. As can be seen, the problem converges after more than 1400 iterations. All simulations are performed with the second-order precision with the help of the SIMPLE algorithm.

## 7. Results and discussion

### *7.1. 1 Streamlines and isotherm-lines for various dimensionless angular velocities*

Fig. 5 shows the contours of streamlines and isotherm-lines for various dimensionless angular velocities. As can be seen, the min-

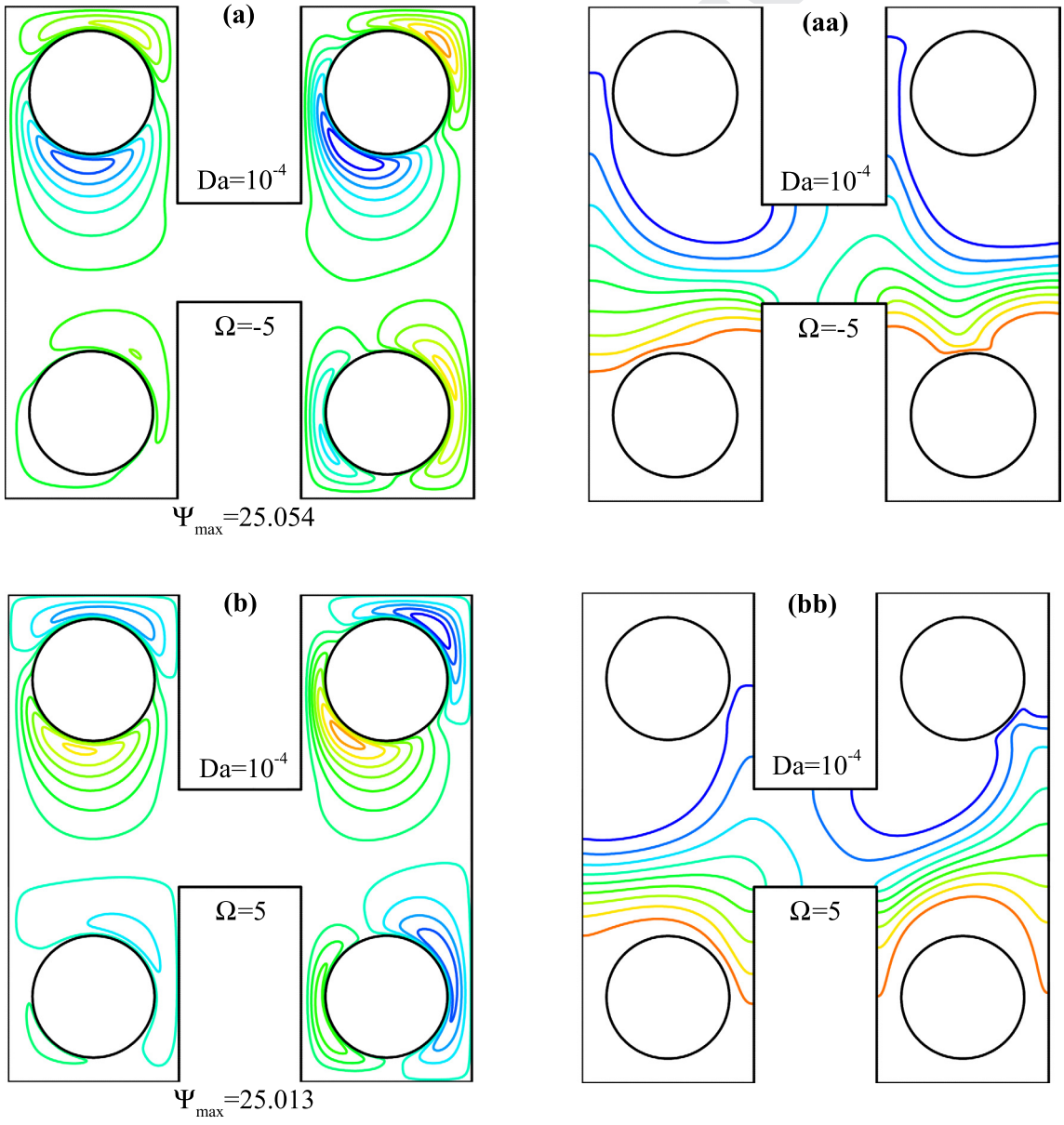


**Fig. 8.** Streamlines (left) and isotherm-lines (right) contours for various Darcy numbers.

Please cite this article as: Z. Li, P. Barnoon, D. Toghraie et al., Mixed convection of non-Newtonian nanofluid in an H-shaped cavity with cooler and heater cylinders filled by a porous material: Two phase approach, Advanced Powder Technology, https://doi.org/10.1016/j.apt.2019.08.014

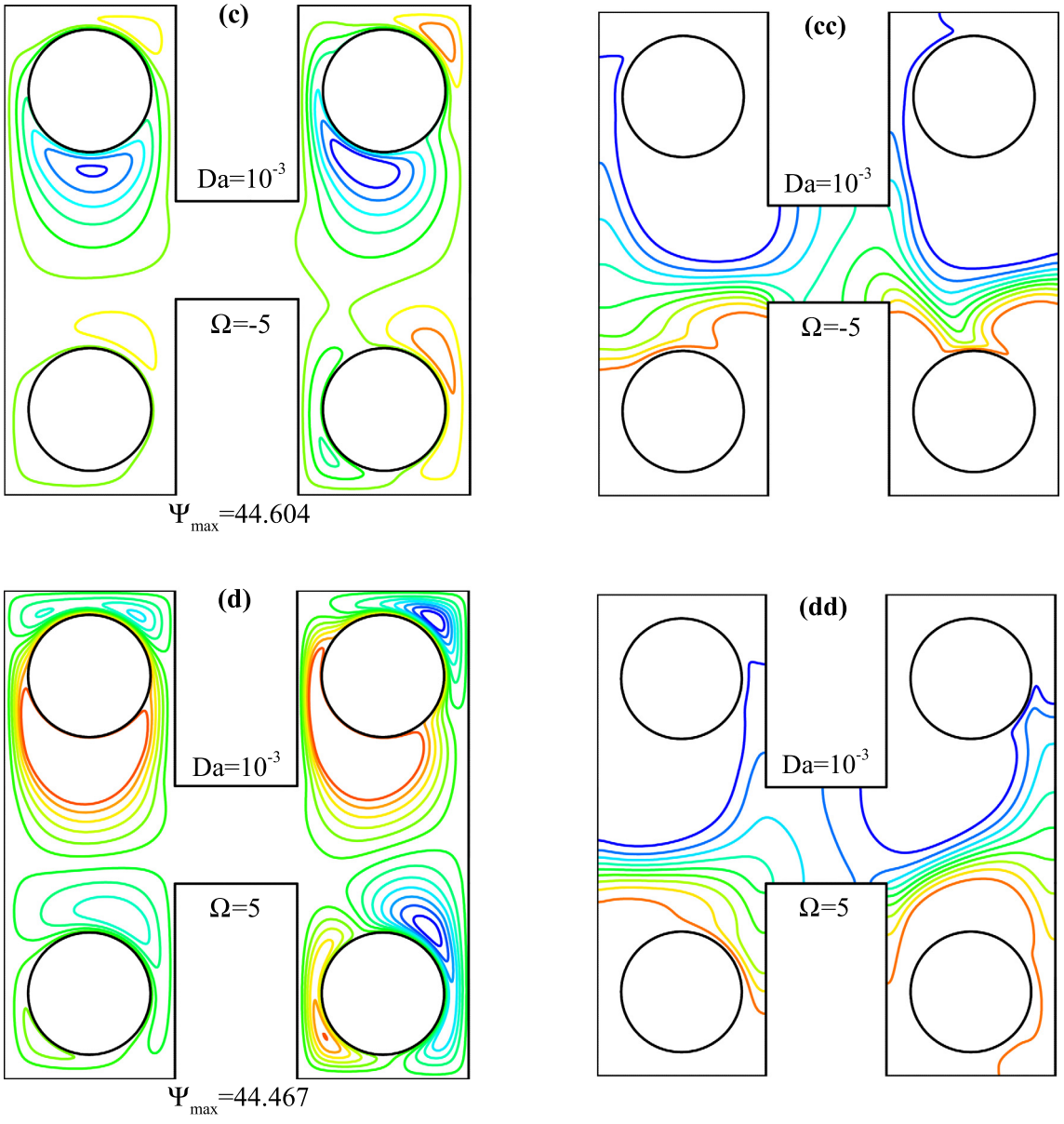


**Fig. 8** (*continued*)

imum value of the stream function occurs at minimum angular velocity. In addition, in all cases, the minimum value of the stream function for a positive angular velocity occurs. When the cylinders are rotated, vortices around the cylinders are formed. The area of the generated vortices for cold cylinders is greater than the hot cylinders, but the power of the generated vortices by the hot cylinders is higher than the cold cylinders. By increasing the angular velocity of the cylinders, the vortex width increases further, so that at the maximum velocity, the flow of the downstream and upstream of the cavity leads to integration. The above process is clearly seen in negative angular velocity. For a positive angular velocity, the process is repeated, except that the flow integration occurs at $\Omega = 5$. As the angular velocity of the cylinder increases, heat dissipation occurs in the cavity and the isotherm-lines appear in the cavity in a non-uniform manner. The heat transfer is done because of the direction of rotation of the cylinders from the left-hand side of the cavity. However, due to the positive angular velocity, the heat dissipation in the cavity is made from the right side of the cavity with less intensity.

### 7.2. Velocity vectors for various angular velocities

Fig. 6 shows the velocity vectors inside the cavity at different angular velocities. As can be seen, the density of velocity vectors adjacent to the cylinders and in the center of the cavity is maximal and minimal. This is due to the fact that in the area in which the cylinders are rotated, there is a amplification of the current in that area, which increases the velocity of the vector and eventually maximizes the velocity in that area. On the other hand, the angular velocity of the cylinders leads to the increase of the flow throughout the cavity. In fact, the angular velocity of the cylinders leads to the maximum velocity in the vicinity of the cylinders and increases

Please cite this article as: Z. Li, P. Barnoon, D. Toghraie et al., Mixed convection of non-Newtonian nanofluid in an H-shaped cavity with cooler and heater cylinders filled by a porous material: Two phase approach, Advanced Powder Technology, https://doi.org/10.1016/j.apt.2019.08.014

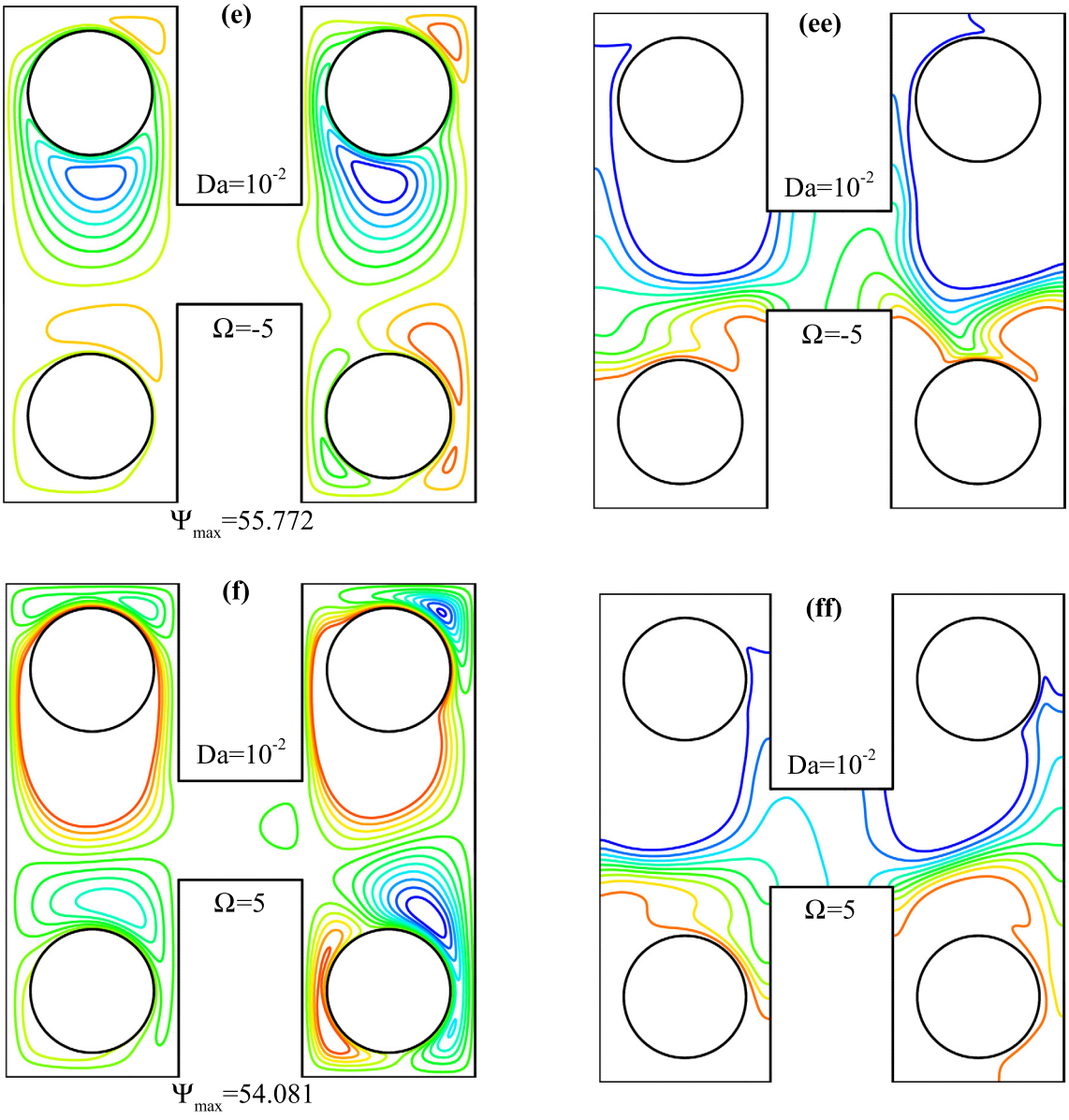


**Fig. 8** (*continued*)

the velocity maximum area. When the cylinders are rotating in the negative or positive direction, the velocity vectors in the vicinity of the cylinders are opposite. The magnification of the velocity vectors is shown in the figure as the cylinders are rotating in a positive and a negative direction. On the other hand, in some areas adjacent to the cylinders, the speed in some areas is maximum and minimum. When the direction of flow rotation inside the cavity is aligned with the direction of cylinder rotation, the velocity in that area is maximized and it can be amplified. But when the direction of flow rotation in the cavity is not aligned with the direction of cylinder rotation, the opposing force causes the velocity field to be neutralized in that area.

### *7.3. Streamlines and isotherm-lines for various aspect ratios*

Fig. 7 shows the contours of the stream lines and the isotherm-lines for various aspect ratios of the cavity. As can be seen, for a negative angular velocity, the turbulences in the cavity decrease with increasing aspect ratio. This means that increasing the aspect ratio to the formation of new vortices that can be due to the integration of the flow in the cavity does not help, but it transforms the area into a calm region. This is even happening for a positive angular velocity. Therefore, increasing the aspect ratio is completely independent of the direction of rotation of the cylinders. Increasing the aspect ratio can lead to a decrease or increase of the stream function, but the amount of changes in the stream function is not significant. In other words, the aspect ratio has had the greatest impact on the magnitude of the flow and extent of generation vortices. Increasing the aspect ratio creates the same behavior for the isotherm-lines. This means that by increasing the aspect ratio, the isotherm lines tend to the center of the cavity, which ultimately leads to lower heat dissipation in the cavity. Increasing the aspect ratio leads to a softening of the isotherm-lines resulting in a decrease in the heat exchange region.

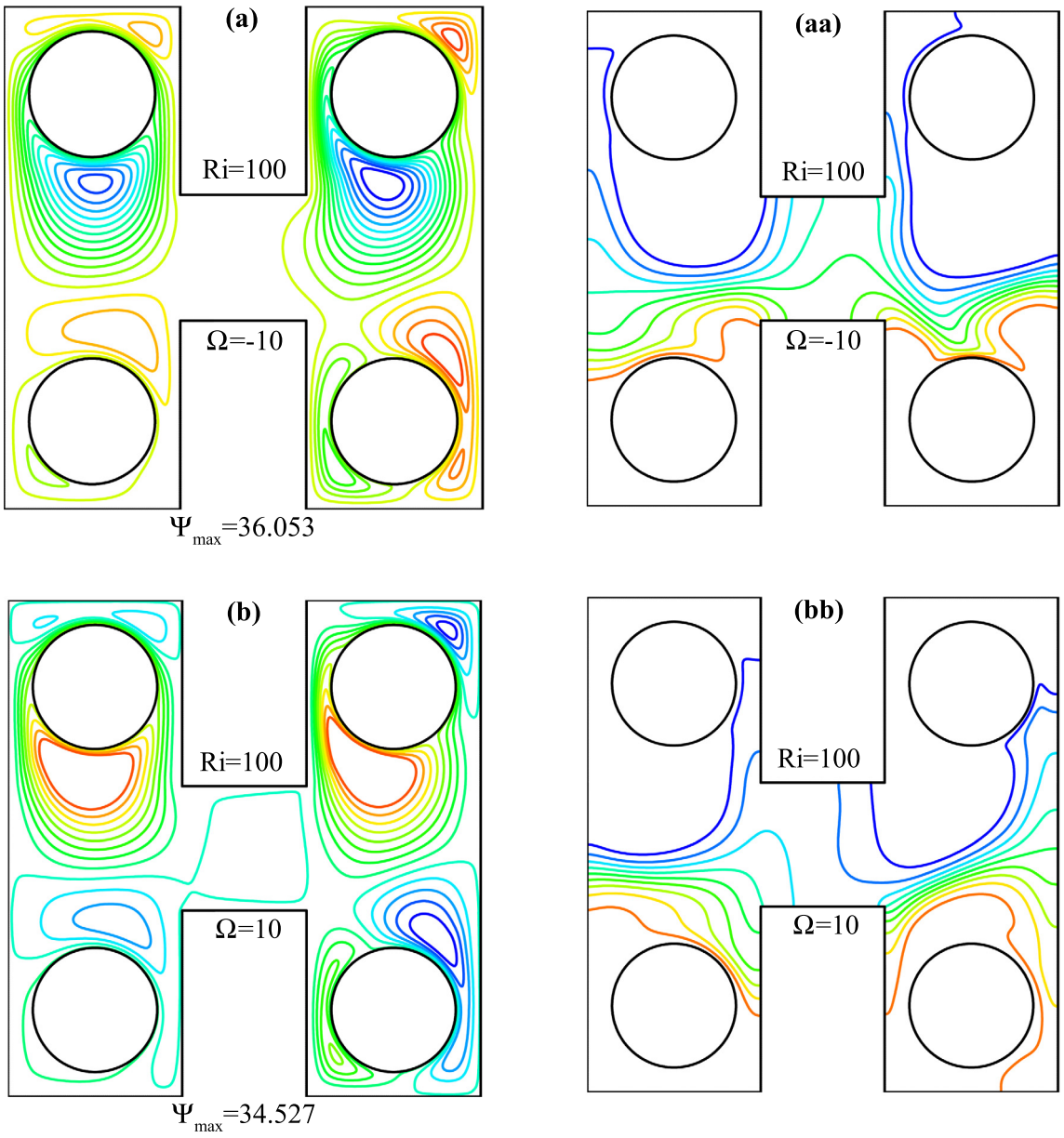


**Fig. 9.** Streamlines (left) and isotherm-lines (right) contours for various Richardson numbers.

### 7.4. Streamlines and isotherm-lines for various Da numbers

Fig. 8 shows the contours of the stream lines and the isotherm-lines for the variation of the Darcy number. For negative angular velocities, with increasing the Darcy number, the stream function increases considerably. In fact, increasing the Darcy number leads to a better fluid flow in the cavity and ultimately leads to an increase in the stream function. The above-mentioned factor leads to the non-equilibrium of the flow field and causes the formation of new vortices in the cavity. For Da = $10^{-3}$ the generated vortices from the cylinders are merged from the right hand of the cavity and lead to the formation of a strong region of flow in the entire cavity. For positive angular velocity, the power and extent of vortices increase in Da = $10^{-3}$ suddenly, so that the maximum vortex strength in the cavity occurs adjacent to cold cylinders. By increasing the Darcy number, the power and extent of the vortex are increased, so that the generated current can absorb by the downstream of the flow completely. By increasing the Darcy number, the streamlines move toward the cylinders, which can lead to increased heat transfer. In fact, the reduction of the Darcy number leads to less permeability in the cavity, which means that the porous matrix surrounds the surface of the cavity, which exacerbates the behavior of the heat conduction in the cavity, and ultimately heat releases in the cavity.

### 7.5. Streamlines and isotherm-lines for various Ri numbers

Fig. 9 shows the contours of the streamlines and isotherm-lines for different Richardson numbers. As can be seen, with the reduction of the Richardson number, the stream function increases considerably. In fact, the increase in the stream function is due to the domination of the forced convection and thus the increase of iner-

Please cite this article as: Z. Li, P. Barnoon, D. Toghraie et al., Mixed convection of non-Newtonian nanofluid in an H-shaped cavity with cooler and heater cylinders filled by a porous material: Two phase approach, Advanced Powder Technology, https://doi.org/10.1016/j.apt.2019.08.014

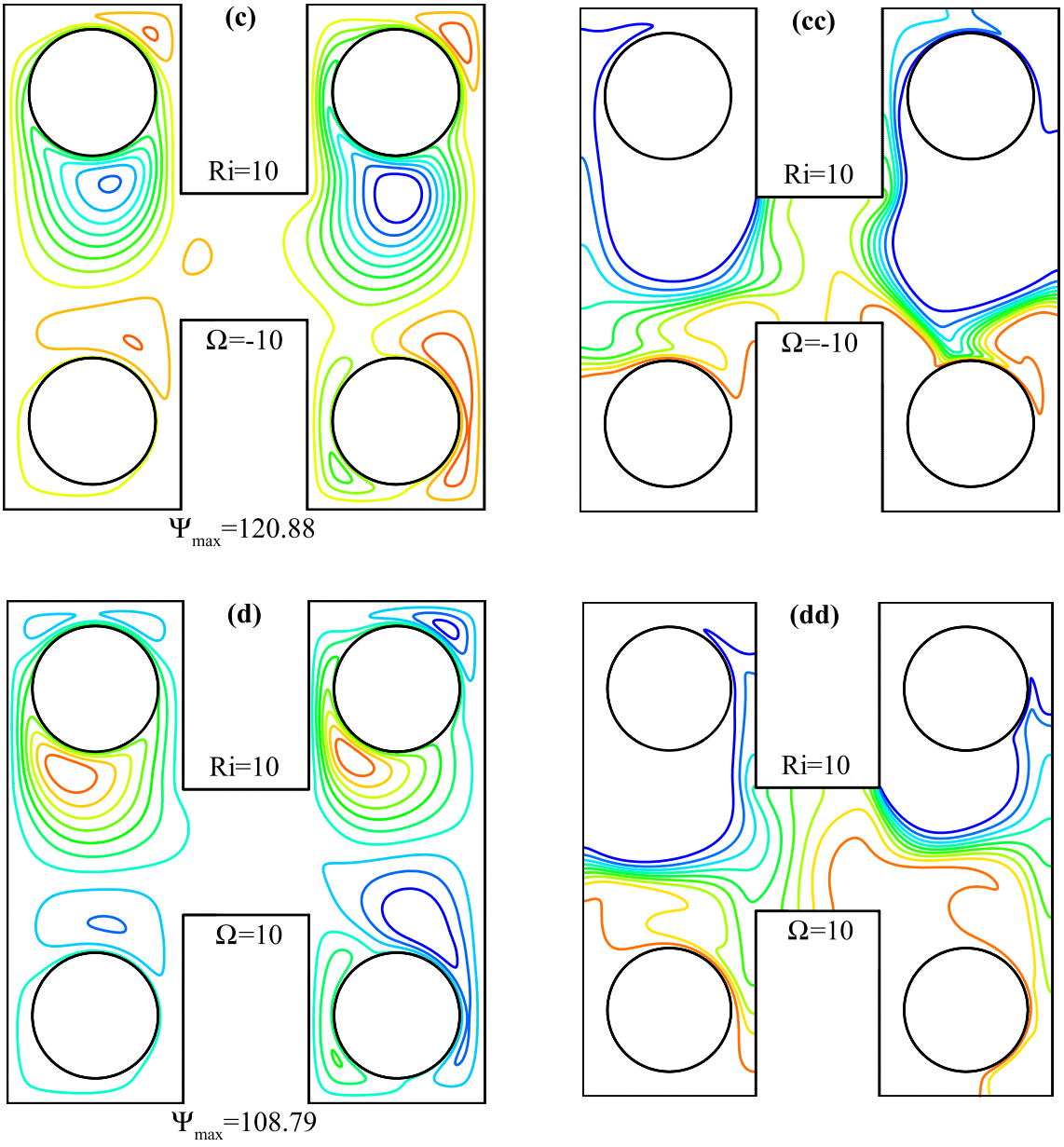


**Fig. 9** (*continued*)

tia. Reducing the Richardson number only leads to power increased. This can even lead to the transmission of vortices when forced convection is dominant noticeably. The phenomena mentioned are true only for negative angular velocity. When a positive angular velocity is considered, in addition to increasing the vortex power and its transmission, increasing the size and integration of vortices is also observed. Reducing the Richardson number leads to a more uneven isotherm-line. For the angular velocity of negative or positive, the above factor is observed. The greatest changes in the isotherm-lines occur in the center of the cavity, which is due to the effects of the rotation of the cylinders on each other. Of course, given the contours of isotherm-lines, it can be seen that even in Ri = 10; the forced convection is not dominant significantly. With the reduction of the Richardson number, forced convection is clearly evident, so that in this case, the heat upstream of the cold and downstream cylinders of the hot cylinders progresses and full heat interconnection is generated.

### 7.6. Effect of aspect raio on heat trasnfer

Fig. 10 illustrates the average Nusselt number in terms of the aspect ratio for various volume fractions. As can be seen, in all cases, the heat transfer is reduced by increasing the aspect ratio. In fact, the increase in the aspect ratio leads to a decrease in the area of heat exchange, and the fluid flow circulation in the cavity becomes more limited, so the flow rate is reduced and the heat transfer decreases eventually. Since the presence of nanoparticles inside the base fluid is a factor for increasing the thermal conductivity, the heat transfer is increased by increasing the volume fraction. In all cases, when the negative angular velocity is considered,

Please cite this article as: Z. Li, P. Barnoon, D. Toghraie et al., Mixed convection of non-Newtonian nanofluid in an H-shaped cavity with cooler and heater cylinders filled by a porous material: Two phase approach, Advanced Powder Technology, https://doi.org/10.1016/j.apt.2019.08.014

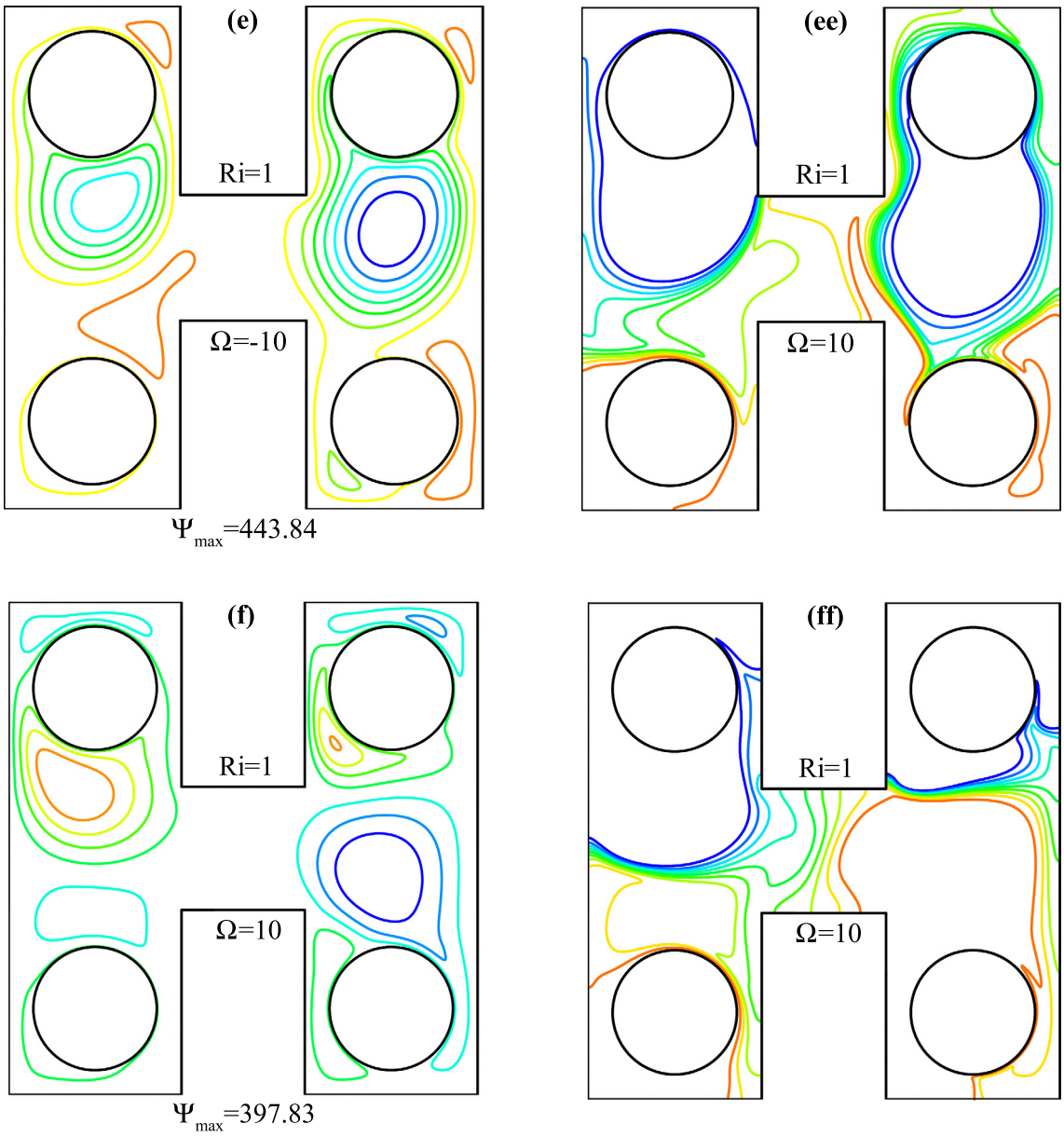


**Fig. 9** (*continued*)

the heat transfer rate is higher than the positive angular velocity. This is due to an increase in thermal gradients in the vicinity of the hot wall. As for the minimum aspect ratio, the percentage of heat transfer at the maximum volume fraction for a negative angular velocity is more than 3.7% relative to the positive angular velocity.

### 7.7. Effect of angular velocity on heat trasnfer

Fig. 11 illustrates the average Nusselt number diagram in terms of the dimensionless angular velocity for different Darcy numbers. As can be seen, the graph's behavior is in the form of zigzag lines. The behavior of the porous medium is highly dependent on the direction of rotation of the cylinders. In high permeability, the use of large negative angular velocities has a better heat transfer than a positive angular velocity. As in $Da = 10^{-2}$, the heat transfer rate is about 9%. Of course, the effect of rotation of cylinders on the heat transfer rate at low permeability is not very significant and can be ignored. In low permeability, the effect of rotating cylinders on the heat transfer rate is significant only when using angular velocities that are large enough. However, if for any reason it is not possible to use large velocities in the design of the system; high permeability can be used to compensate for the increase of heat transfer with the aid of this case.

### 7.8. Effect of Ri number on heat trasnfer

Fig. 12 illustrates the average Nusselt number in terms of the Richardson number for different angular velocities. As can be seen, the lowest amount of heat transfer is related to the state of natural convection. Therefore, the use of the mixed convection mechanism can play a significant role in increasing the heat transfer rate. So that in Richardson's maximum (even when forced convection is not significantly) there is a 60% increase in heat transfer rate relative to the natural convection. Also, increasing the angular velocity of the cylinders, the heat transfer rate increases. In fact, the angular

Please cite this article as: Z. Li, P. Barnoon, D. Toghraie et al., Mixed convection of non-Newtonian nanofluid in an H-shaped cavity with cooler and heater cylinders filled by a porous material: Two phase approach, Advanced Powder Technology, https://doi.org/10.1016/j.apt.2019.08.014

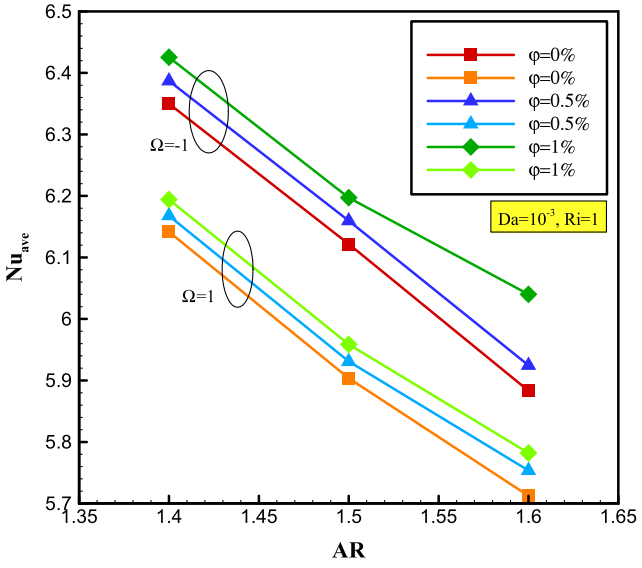


**Fig. 10.** Nusselt number versus aspect ratio for various voulme fractions.

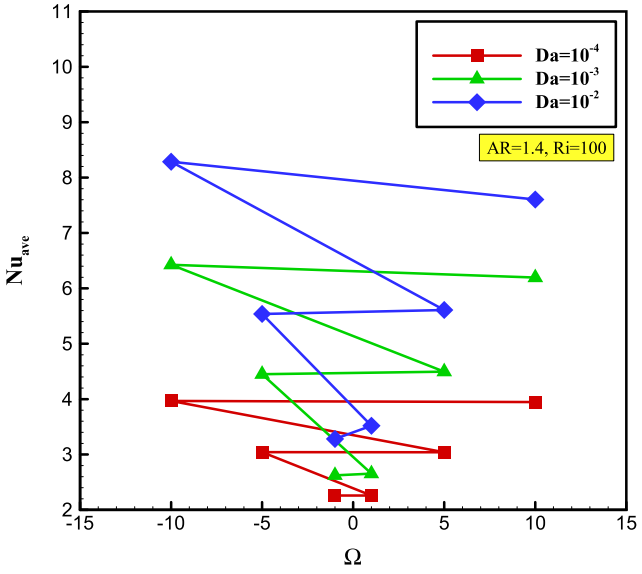


**Fig. 11.** Nusselt number vs dimensionless angular velocity for various Darcy numbers.

velocity of the cylinders leads to a better fluid flow circulation in the cavity and leads to an intensification of the gradient of velocity and thermal gradients in the vicinity of the hot wall, which ultimately leads to an increase in the heat transfer rate. The angular velocity of the cylinders is closely related with increasing convection forces and the heat transfer rate, so as the convection forces increase, the slope of the graph becomes more intense. Therefore, in a constant Richardson number, changes in the heat transfer rate are very high and the intensity of these changes increases with the increase of forced convection. In Ri = 1, there is an increase of 219% of the heat transfer rate by 10 times the angular velocity. However, in Ri = 100, an increase of 116% is achieved by a 10 times increase in the angular velocity.

## 8. Conclusion

In this study, mixed convection of a non-Newtonian nanofluid in a permeable H-shape enclosure using a two-phase model was investigated. The results that can be taken include:

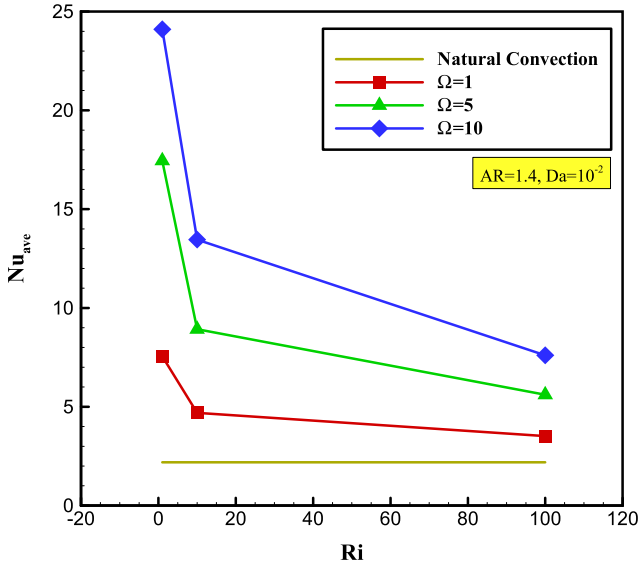


**Fig. 12.** Nusselt number versus Richardson number for various dimensionless angular velocity.

- As the aspect ratio increases, the heat transfer rate decreases. Increasing the aspect ratio leads to reduced generation vortices.
- Increasing the Darcy number and decreasing the Richardson number, the heat transfer rate increases.
- The direction of cylinders rotation affects the heat transfer rate and the formation of fluid flow in the cavity.
- In low permeability, the effect of rotating cylinders on the heat transfer rate is significant only when using angular velocities that are large enough.
- If for any reason, it is not possible to use large velocities in the design of the system, high permeability can be used to compensate for the increase of heat transfer with the help of this case.

## Acknowledgement

This research is partially supported by Key Laboratory of Fluid Power and Intelligent Electro-Hydraulic Control (Fuzhou University).

## References

[1] X. Qi Wang, A.S. Mujumdar, A review on nanofluids - part II: experiments and applications, Braz. J. Chem. Eng. 25 (4) (2008) 631–648.
[2] L. Godson, B. Raja, D.M. Lal, S. Wongwises, Enhancement of heat transfer using nanofluids—an overview, Renew. Sust. Energy Rev. 14 (2010) 629–641.
[3] L. Cheng, Nanofluid heat transfer technologies, Recent Pat. Chem. Eng. 3 (1) (2009) 1–7.
[4] Si-Ning Li, Hong-Na Zhang, Xiao-Bin Li, Qian Li, Feng-Chen Li, Shizhi Qian, Sang Woo Joo, Numerical study on the heat transfer performance of non-Newtonian fluid flow in a manifold microchannel heat sink, Appl. Therm. Eng. 115 (2017) 1213–1225.
[5] P. Barnoon, D. Toghraie, Numerical investigation of laminar flow and heat transfer of non-Newtonian nanofluid within a porous medium, Powder Technol. 325 (2018) 78–91.
[6] R. Daghigh, P. Zandi, Experimental analysis of heat transfer in spiral coils using nanofluids and coil geometry change in a solar system, Appl. Therm. Eng. 145 (2018) 295–304.
[7] Z. Mehrez, M. Bouterra, A.E. Cafsi, A. Belghith, Heat transfer and entropy generation analysis of nanofluids flow in an open cavity, Comput. Fluids 88 (2013) 363–373.
[8] SY Ahmed, F Hassan Ali, H K Hamzah, Heatlines Visualization of Natural Convection in Trapezoidal Cavity Filled with Nanofluid and Divided by Porous Medium Partition, Comput. Fluids, https://doi.org/10.1016/j.compfluid.2018.12.004.

Please cite this article as: Z. Li, P. Barnoon, D. Toghraie et al., Mixed convection of non-Newtonian nanofluid in an H-shaped cavity with cooler and heater cylinders filled by a porous material: Two phase approach, Advanced Powder Technology, https://doi.org/10.1016/j.apt.2019.08.014

[9] M. Hosseini Abadshapoori, M.H. Saidi, Lattice Boltzmann simulation of TiO2-water nanofluid in a curved boundary domain at high Rayleigh numbers, Comput. Fluids 168 (2018) 159–169.
[10] B. Mahdi Al-Srayyih, S. Sh Gao, Hadi Hussain, Effects of linearly heated left wall on natural convection within a superposed cavity filled with composite nanofluid-porous layers, Adv. Powder Technol. 30 (2019) 55–72.
[11] R. Yaghoubi Emami, M. Siavashi, Gh Shahriari Moghaddam, The effect of inclination angle and hot wall configuration on Cu-water nanofluid natural convection inside a porous square cavity, Adv. Powder Technol. 29 (2018) 519–536.
[12] M. Rajarathinam, N. Nithyadevi, Ali J. Chamkha, Heat transfer enhancement of mixed convection in an inclined porous cavity using Cu-water nanofluid, Adv. Powder Technol. 29 (2018) 590–605.
[13] I. Hashim, A.I. Alsabery, M.A. Sheremet, A.J. Chamkha, Numerical investigation of natural convection of Al2O3-water nanofluid in a wavy cavity with conductive inner block using Buongiorno's two-phase model, Adv. Powder Technol. 30 (2019) 399–414.
[14] Ching-Chang Cho, Mixed convection heat transfer and entropy generation of Cu-water nanofluid in wavy-wall lid-driven cavity in presence of inclined magnetic field, Int. J. Mech. Sci. 151 (2019) 703–714.
[15] L. Wang, Xu Yang, C. Huang, Zh Chai, B. Shi, Hybrid lattice Boltzmann-TVD simulation of natural convection of nanofluids in a partially heated square cavity using Buongiorno's model, Appl. Therm. Eng. 146 (2019) 318–327.
[16] Abdullah A.A.A. Al-Rashed, Amin Shahsavar, Mohammad Akbari, Davood Toghraie, Masoud Afrand, Finite Volume Simulation of mixed convection in an inclined lid-driven cavity filled with nanofluids: Effects of a hot elliptical centric cylinder, cavity angle and volume fraction of nanoparticles, Phys. A (Amsterdam, Neth.), https://doi.org/10.1016/j.physa.2019.121122.
[17] A. Baïri, Natural convection between concentric and inclined hemispherical cavities filled with Cu-water nanofluid, J. Mol. Liq. 249 (2018) 1263–1270.
[18] S. Baghsaz, S. Rezanejad, M. Moghimi, Numerical investigation of transient natural convection and entropy generation analysis in a porous cavity filled with nanofluid considering nanoparticles sedimentation, J. Mol. Liq. 279 (2019) 327–341.
[19] Y.J. Zhuang, Q.Y. Zhu, Numerical study on combined buoyancy–Marangoni convection heat and mass transfer of power-law nanofluids in a cubic cavity filled with a heterogeneous porous medium, Int. J. Heat Fluid Flow 71 (2018) 39–54.
[20] Yi-Ying Bao, Jia-Hui Huang, Yan-Jun Chen, Zhen-Hua Liu, Natural convection heat transfer of nanofluid in a cavity under an inhomogeneous electric field, Int. J. Heat Mass Trans. 131 (2019) 341–345.
[21] P. Barnoon, D. Toghraie, R. Balali Dehkordi, H. Abed, MHD mixed convection and entropy generation in a lid-driven cavity with rotating cylinders filled by a nanofluid using two phase mixture model, J. Magn. Magn. Mater. 483 (2019) 224–248.
[22] P. Barnoon, D. Toghraie, F. Eslami, B. Mehmandoust, Entropy generation analysis of different nanofluid flows in the space between two concentric horizontal pipes in the presence of magnetic field: Single-phase and two-phase approaches, Com. Math. App. 77 (2019) 662–692.
[23] M. Hatami, J. Zhou, J. Geng, D. Song, D. Jing, Optimization of a lid-driven T-shaped porous cavity to improve the nanofluids mixed convection heat transfer, J. Mol. Liq. 231 (2017) 620–631.
[24] E. Khalili, A. Saboonchi, M. Saghafian, Experimental study of nanoparticles distribution in natural convection of Al2O3-water nanofluid in a square cavity, Int. J. Therm. Sci. 112 (2017) 82–91.
[25] O. Mahian, A. Kianifar, S. Zeinali Heris, S. Wongwises, Natural convection of silica nanofluids in square and triangular enclosures: Theoretical and experimental study, Int. J. Heat Mass Trans. 99 (2016) 792–804.
[26] B. Ruhani, P. Barnoon, D. Toghraie, Statistical investigation for developing a new model for rheological behavior of Silica–ethylene glycol/Water hybrid Newtonian nanofluid using experimental data, Phys. A (Amsterdam, Neth.) 525 (2019) 616–627.
[27] A.I. Rahimi, A. Kasaeipoor, E. Hasani Malekshah, L. Kolsi, Experimental and numerical study on heat transfer performance of three-dimensional natural convection in an enclosure filled with DWCNTs-water nanofluid, Powder Technol. 322 (2017) 340–352.
[28] S. Osman, M. Sharifpur, J.P. Meyer, Experimental investigation of convection heat transfer in the transition flow regime of aluminium oxide-water nanofluids in a rectangular channel, Int. J. Heat Mass Trans. 133 (2019) 895–902.
[29] M. Khoshvaght-Aliabadi, S. Deldar, S.M. Hassani, Effects of pin-fins geometry and nanofluid on the performance of a pin-fin miniature heat sink (PFMHS), Int. J. Mech. Sci. 148 (2018) 442–458.
[30] A. Rahimi, A. Kasaeipoor, E. Hasani Malekshah, l. kolsi, Natural convection analysis by entropy generation and heatline visualization using lattice Boltzmann method in nanofluid filled cavity included with internal heaters-Empirical thermo-physical properties, Int. J. Mech. Sci. 133 (2017) 199–216.
[31] M. Manninen, V. Taivassalo, S. Kallio, On the mixture model for multiphase flow, Tech. Res. Cent. Finland Finland (1996).
[32] L. Schiller, A. Naumann, A drag coefficient correlation, Vdi Zeitung 77 (1935) 51.
[33] J.C. Maxwell, Treatise on Electricity and Magnetism, Clarendon Press, Oxford, 1873.
[34] H. Brinkman, The viscosity of concentrated suspensions and solutions, J. Chem. Phys. 20 (1952) 571–577.
[35] B.C. Pak, Y.1. Cho, Hydrodynamic and heat transfer study of dispersed fluids with submicron metallic oxide particles, Exp. Heat Trans. Int. J. 11 (2) (1998) 141–170.
[36] Y. Xuan, W. Roetzel, Conceptions for heat transfer correlation of nanofluids, Int. J. Heat Mass Trans. 43 (19) (2000) 3701–3707.
[37] K. Khanafer, S.M. Aithal, Laminar mixed convection flow and heat transfer characteristics in a lid driven cavity with a circular cylinder, Int. J. Heat Mass Trans. 66 (2013) 200–209.
[38] C.J. Ho, W.K. Liu, C.C. Lin, Natural convection heat transfer of alumina-water nanofluid invertical square enclosures: an experimental study, Int. J. Therm. Sci. 49 (2010) 1345–1353.
[39] S.Y. Motlagh, H. Soltanipour, Natural convection of Al2O3-water nanofluid in an inclined cavity using Buongiorno's two-phase model, Int. J. Therm. Sci. 111 (2017) 310–320.
[40] P. Nithiarasu, K.N. Seetharamu, T. Sundararajan, Natural convective heat transfer in a fluid saturated variable porosity medium, Int. J. Heat Man Trans. 40 (16) (1997) 3955–3967.
[41] Abdullah A.A.A. Al-Rashed, A. Shahsavar, S. Entezari, M.A. Moghimi, T.K. Nguyen, Numerical investigation of non-Newtonian water-CMC/CuO nanofluid flow in an offset strip-fin microchannel heat sink: Thermal performance and thermodynamic considerations, Appl. Therm. Eng. 155 (2019) 247–258.
[42] T.K. Nguyen, A. Saidizad, M. Jafaryar, M. Sheikholeslami, Zh. Li, Influence of various shapes of CuO nanomaterial on nanofluid forced convection within a sinusoidal channel with obstacles, Chem. Eng. Res. Des. 146 (2019) 478–485.
[43] A.M. Rashad, M.M. Rashidi, G. Lorenzini, S.E. Ahmed, A.M. Aly, Magnetic field and internal heat generation effects on the free convection in a rectangular cavity filled with a porous medium saturated with Cu–water nanofluid, Int. J. Heat Mass Trans. 104 (2017) 878–889.
[44] N. Freidoonimehr, M.M. Rashidi, S. Mahmud, Unsteady MHD free convective flow past a permeable stretching vertical surface in a nano-fluid, Int. J. Therm. Sci. 87 (2015) 136–145.
[45] M. Sheikholeslami, M.M. Rashidi, D.D. Ganji, Effect of non-uniform magnetic field on forced convection heat transfer of $Fe_3O_4$ –water nanofluid, Comput Meth Appl Mech Eng. 294 (2015) 299–312.
[46] F. Garoosi, L. Jahanshaloo, M.M. Rashidi, A. Badakhsh, M.E. Alie, Numerical simulation of natural convection of the nanofluid in heat exchangers using a Buongiorno model, Appl Math Comput 254 (2015) 183–203.
[47] M.M. Bhatti, S.R. Mishra, T. Abbas, M.M. Rashidi, A mathematical model of MHD nanofluid flow having gyrotactic microorganisms with thermal radiation and chemical reaction effects, Neural Comput. Appl. 30 (2018) 1237–1249.
[48] M.A. Ismael, T. Armaghani, A.J. Chamkha, Conjugate heat transfer and entropy generation in a cavity filled with a nanofluid-saturated porous media and heated by a triangular solid, J. Taiwan Inst. Chem. Eng. 59 (2016) 138–151.
[49] A.J. Chamkha, H. Al-Naser, Double-diffusive convection in an inclined porous enclosure with opposing temperature and concentration gradients, Int. J. Therm. Sci. 40 (2001) 227–244.
[50] A.J. Chamkha, M.A. Mansour, S.E. Ahmed, Double-diffusive natural convection in inclined finned triangular porous enclosures in the presence of heat generation/absorption effects, Heat Mass Trans. 46 (2010) 757–768.
[51] J.C. Umavathi, J.P. Kumar, A.J. Chamkha, I. Pop, Mixed convection in a vertical porous channel, Trans. Porous Media 61 (2005) 315–335.
[52] R. Nasrin, M.A. Alim, A.J. Chamkha, Combined convection flow in triangular wavy chamber filled with water–CuO nanofluid: effect of viscosity models, Int. Commun. Heat Mass Trans. 39 (2012) 1226–1236.
[53] M.A. Ismael, I. Pop, A.J. Chamkha, Mixed convection in a lid-driven square cavity with partial slip, Int. J. Therm. Sci. 82 (2014) 47–61.
[54] A.J. Chamkha, M.A. Ismael, Conjugate heat transfer in a porous cavity heated by a triangular thick wall, Numer. Heat Trans. Part A 63 (2013) 144–158.
[55] S. Parvin, A.J. Chamkha, An analysis on free convection flow, heat transfer and entropy generation in an odd-shaped cavity filled with nanofluid, Int. Commun. Heat Mass Trans. 54 (2014) 8–17.
[56] A.J. Chamkha, M.A. Ismael, Natural convection in differentially heated partially porous layered cavities filled with a nanofluid, Numer. Heat Trans. Part A 65 (2014) 1089–1113.
[57] S. Parvin, R. Nasrin, M.A. Alim, N.F. Hossain, A.J. Chamkha, Thermal conductivity variation on natural convection flow of water–alumina nanofluid in an annulus, Int. J. Heat Mass Trans. 55 (2012) 5268–5274.
[58] A.J. Chamkha, Non-Darcy fully developed mixed convection in a porous medium channel with heat generation/absorption and hydromagnetic effects, Numer. Heat Trans. Part A 32 (1997) 653–675.
[59] A.I. Alsabery, A.J. Chamkha, H. Saleh, I. Hashim, Natural convection flow of a nanofluid in an inclined square enclosure partially filled with a porous medium, Scientific Reports 2357 (2017).
[60] A.J. Chamkha, A.R.A. Khaled, Similarity solutions for hydromagnetic mixed convection heat and mass transfer for Hiemenz flow through porous media, Int. J. Numer. Methods Heat Fluid Flow 10 (2000) 94–115.
[61] A.J. Chamkha, Unsteady laminar hydromagnetic fluid–particle flow and heat transfer in channels and circular pipes, Int. J. Heat Fluid Flow 21 (2000) 740–746.
[62] A.J. Chamkha, On laminar hydromagnetic mixed convection flow in a vertical channel with symmetric and asymmetric wall heating conditions, Int. J. Heat Mass Trans. 45 (2002) 2509–2525.



Please cite this article as: Z. Li, P. Barnoon, D. Toghraie et al., Mixed convection of non-Newtonian nanofluid in an H-shaped cavity with cooler and heater cylinders filled by a porous material: Two phase approach, Advanced Powder Technology, https://doi.org/10.1016/j.apt.2019.08.014